

Chapter 1

Carbon Materials From Various Sources for Composite Materials



Zhipeng Wang, Karen Wong Min Jin, and Gan Jet Hong Melvin

1.1 Introduction

Carbon material can be considered as a versatile material which is widely utilized in research development and industrial/commercial applications. Carbon materials can be in various forms; carbon nanotube (CNT), graphene, carbon black, activated carbon, graphite whisker, fullerene, and many more. Most of the carbon materials mentioned, possess significant mechanical, electrical, thermal, and chemical properties, which allow them to be utilized in diverse fields such as composite materials, energy storage/conversion, electronic, optical, sensor, and so on.

For decades the studies of macrocomposites such as reinforced polymers have been conducted intensively, where the length scale of polymer fillers is in micrometers. The reinforcement length scale is in micrometers, and the interface of fillers is close to the bulk polymer matrix (Koo 2006). Conversely, composites that are reinforced with nanometer scale fillers are considered as nanocomposites (Koo 2006; Young and Lovell 2011). Nanocomposites are composite materials in which the matrix material is reinforced by one or more separate nanomaterials in order to improve performance properties (Hu et al. 2010a). The nanocomposites have ultra large interfacial area per volume, and the distances between the polymer and filler components are extremely short. As a result, molecular interaction between the polymer and the nanoparticles (NPs) will give polymer nanocomposites outstanding

Z. Wang
Institute of Advanced Materials, Jiangxi Normal University,
Nanchang City, Jiangxi Province, China
e-mail: wangzhipeng@jxnu.edu.cn

K. W. M. Jin · G. J. H. Melvin (✉)
Material and Mineral Research Unit (MMRU), Faculty of Engineering,
Universiti Malaysia Sabah, Kota Kinabalu, Sabah, Malaysia
e-mail: melvin.gan@ums.edu.my

material properties that conventional polymers do not possess (Koo 2006). Commonly, the matrix materials used for composites are polymers such as polyurethane, epoxy resin, synthetic/natural rubber, polyvinyl alcohol, polyvinyl chloride, paraffin wax, and so on.

Satisfactory range of mechanical, optical, electrical, and surface properties can be obtained from polymers alone (Ober and Müllen 2012). Over the last century, polymers have dynamically transformed technology more than any other materials. Their combination of light weight, low cost, molecular specificity, corrosion resistance, and the properties associated with their large molecular size have made them attractive replacements for metals and ceramics in their role as structural and functional materials (Ober and Müllen 2012). In recent years, the discovery of the electrical, electronic, and optical properties of polymers over the last decade has opened up a vast variety of new applications in enhancing and demanding technologies.

Nevertheless, there are often circumstances where even more specific or better performance is demanded from the polymers. Since the development of polymers, composite have been used to enhance properties or improve them. The formation of the composite involves incorporating filler, commonly an inorganic filler, to modify polymer performance. In recent years, very small scale fillers, some having dimensions of just a few nanometers, have been modulated to fabricate nanocomposites.

The development of composites has been driven by the need for materials with specific combinations of properties beyond those obtainable from a single material (Young and Lovell 2011). The incorporation of inorganic nanoparticles as the fillers into polymer systems has resulted in polymer nanocomposites showing multifunctional, high performance polymer characteristics further than those traditional filled polymeric materials possess (Koo 2006; Hu et al. 2010a; Schaefer and Justice 2007; Thostenson et al. 2005). Through control or alteration of the fillers at the nanoscale level, we will be able to maximize property enhancement of selected polymer systems to meet or exceed the requirements of current military, aerospace, commercial applications, and so on (Koo 2006). The technical approach involves the incorporation of nanoparticles into selected polymer systems whereby nanoparticles may be surface-treated to provide good dispersion and enhanced inclusion into polymer matrix.

1.2 Carbon-Based Composite Materials

1.2.1 Carbon Nanotube-Based Composite Materials

Huge numbers of research and development of CNTs, from history, synthesis, remarkable performances, and fabrication of CNT-based nanocomposites, are available. The enhancement and great attention to CNTs can be highlighted when Kroto et al. (1985) discovered fullerene (C₆₀, buckyball); Oberlin et al. (1976) synthesized

among the first CNTs; multi- (Iijima 1991) and single-walled (Iijima and Ichihashi 1993) CNTs were observed; which keep on developing up to today.

In general, CNTs can be categorized into single-walled CNT (SWCNT) and multi-walled CNT (MWCNT). A SWCNT can be considered as a rolled-up sheet of a graphene, which is a single layer of an allotrope of carbon called graphite, and the edges of the sheet are joined together to form a seamless tube (Young and Lovell 2011; Hierold et al. 2008). Few tubes of different diameters can be fitted into each other, which normally classified as MWCNT. Arc discharge, laser ablation, and chemical vapor deposition (CVD) are three major methods to produce CNTs. Each of these methods had its advantages and disadvantages and shortly explained below.

Arc discharge and laser ablation method depends on the evaporation of a graphite target to create gas phase carbon fragments that recombine to form CNTs. During the process, the temperature reached at 2000–3000 °C range, which allows the carbon atoms to rearrange into the tube structure. Normally, in order to promote the yield of CNTs, several different metals in concentrations about 1% are incorporated into the target materials that is evaporated (Hierold et al. 2008). In the case where large quantity of CNTs is necessary for composite materials, these methods would make the cost of CNTs unreasonable (Thostenson et al. 2001). Moreover, purification steps are also essential before the utilization of them, due to a large amount of non-tubular graphitic and amorphous carbon is also yielded during the process (Hierold et al. 2008; Thostenson et al. 2001).

One of the most broadly utilized methods to produce CNTs is CVD. Commonly, the CVD process includes catalyst-assisted decomposition of hydrocarbons, such as ethylene or acetylene, in a tube reactor within 400–1100 °C temperature range and the growth of CNTs over the catalyst upon cooling the system (Hierold et al. 2008; Hu et al. 2010b; Popov 2004). The growth temperature depends on the type of CNTs to be grown and the catalyst composition (Hierold et al. 2008). The advantages of this method are the ability to fabricate aligned arrays of CNTs with controlled diameter and length, and under the right condition only nanotubes can be yielded and no undesired graphitic material (Hierold et al. 2008; Thostenson et al. 2001).

CNTs also can be synthesized from various sources. For example, waste plastic such as polyethylene, polypropylene, and polyethylene terephthalate can be utilized as carbonaceous feed of CNT production (Bazargan A and McKay 2012; Mishra et al. 2012). Moreover, CNTs also can be obtained from coconut shell derived charcoal by using plasma enhanced CVD (Araga and Sharma 2017), and bamboo charcoal by CVD in the presence of ethanol vapor (Zhu et al. 2012). Many renewable carbon-based resources, especially biomasses, have high potential in CNTs production. Few examples are such as solid camphor, camphor oil, palm oil, chicken fat oil, honey, butter, and many more (Kumar et al. 2016; Titirici et al. 2015). The utilization of waste materials, renewable carbon resources, and low cost abundant materials will lead to the environmental friendly synthesis methods and the advancement of sustainable technologies.

Usually, CNTs are incorporated into polymer matrix to fabricate composite materials for various applications. In other cases, CNTs are combined with other

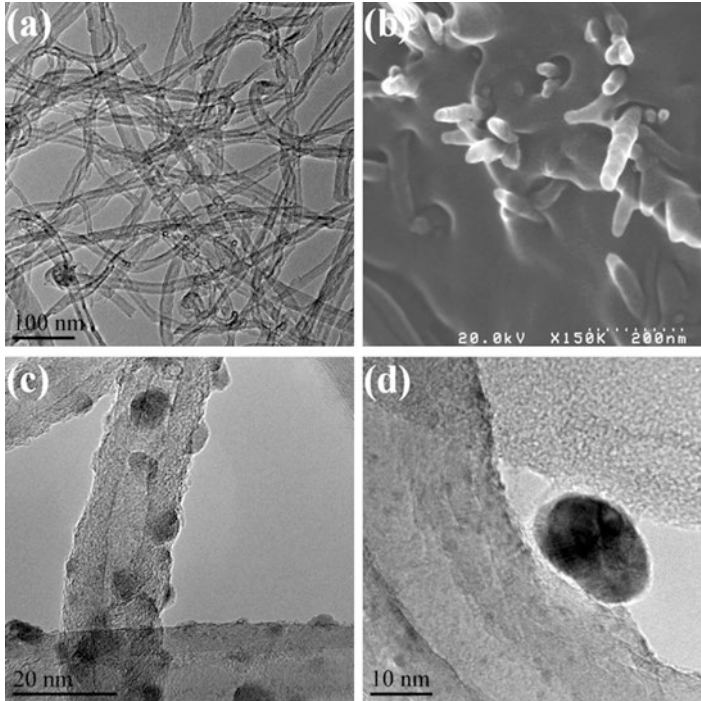


Fig. 1.1 (a) TEM image of MWCNT, (b) FE-SEM image of CNTs incorporated into polymer matrix, TEM images of (c) BaTiO₃/CNT, (d) Ag/CNT

materials to synthesize hybrid nanocomposites. Several CNT-based materials are depicted in Fig. 1.1. Ajayan et al. (1994) conducted one of the first fabrications of polymer nanocomposites using CNTs as fillers. Since then, the development of CNT-based composite materials is growing rapidly, for instance in electromagnetic (EM) wave absorber, electroactive actuator, energy storage devices, advanced materials, and many more applications.

CNTs are favorable candidate to be considered for EM wave absorber composite materials due to their the high electrical conductivity which enables strong polarization to occur, Ohmic losses, dissipation of electrostatic charges, or multiple scattering caused by the large specific area, which lead to enhanced complex permittivity (Melvin et al. 2019a). For example, Nwigboji et al. (2015) fabricated MWCNT-epoxy composites and evaluated their EM wave absorption performance. Significant EM wave absorption can be obtained for 8–10 wt.% samples within the frequency range of 1–26.5 GHz. In order to produce high performance EM wave absorber materials, combination of two/more materials or hybrid materials are desirable, where single material system unable to meet the demand. In this particular case, hybrid materials are referred as CNTs combined with magnetic, dielectric, or conductive particles for EM wave absorber applications. Qiu and Qiu (2015) fabricated magnetite nanoparticle – CNT – hollow carbon fiber composites and evaluated their

EM wave absorption capability. The minimum reflection loss achieved is -50.9 dB at 14.03 GHz for 2.5 mm thick sample layer. CNTs are also combined with dielectric ceramic such as barium titanate (BTO) nanoparticles through solvothermal method (Bi et al. 2011; Huang et al. 2013) and sol-gel method (Melvin et al. 2014a, 2017a), to enhance the absorption performance. It is worth noticing that the EM wave absorption performance can be improved not only by utilizing hybrid materials, but also by modulating the design, such as double-layer BTO/CNT composites (Ni et al. 2015). The double-layer BTO/CNT composites with total thickness of 1.3 mm, consist of BTO/CNT 30 wt.% (absorption layer) and BTO 30 wt.% (matching layer) exhibited minimum reflection loss of -63.7 dB ($> 99.9999\%$ absorption) at 13.7 GHz. Furthermore, CNTs are also integrated with conductive particles such as silver (Ag) nanoparticles, for single (Melvin et al. 2014b) or double-layer Ag/CNT (Melvin et al. 2015) EM wave absorber composite materials. The double-layer composites constructed from CNT 30 wt.% and Ag/CNT 30 wt.% with total thickness of 3.3 mm exhibited minimum reflection of -52.9 dB ($> 99.999\%$ absorption) at 6.3 GHz.

CNTs also can be incorporated into polymer matrix such as polyurethane (PU) to fabricate electroactive nanocomposite actuator. An electric field stimulated polymer-based materials are referred to as electroactive actuators (shape memory polymers) and have the advantages, such as light weight, flexible, tolerance against fracture, easy to fabricate, and they can convert electrical energy to mechanical energy and thus impart a force and produce large strain (Ali and Hirai 2011; Melvin et al. 2016). Moreover, through the inclusion of CNTs, mechanical and electrical properties can be improved significantly, which further make them suitable to be developed for actuator materials, sensors, artificial muscles, smart devices, and micro-switches (Sahoo et al. 2007; Melvin et al. 2014c, d, 2016). For instance, PU/CNT electroactive nanocomposite actuator film bends toward the cathode when an electric field was applied, and it reverted to its original position when the electric field was removed. Stable and similar bending displacement also observed upon voltage cycling (Melvin et al. 2014d). Furthermore, CNT/water-borne epoxy showed triple-shape memory effect when thermally actuated, where normally common epoxy or CNT/epoxy nanocomposites only possess dual-shape memory effect (Dong et al. 2015).

Not limited to those mentioned above, CNT-based composite materials are also widely used as the electrode materials in supercapacitor applications, due to their remarkable physiochemical properties such as high conductivity, high surface area, and electrochemical activity (Wang and Melvin 2019). For instance, CNTs constructed nitrogen-doped porous carbon monoliths for supercapacitor application (Wang et al. 2019c). Furthermore, CNTs are also incorporated into matrix material to fabricate functionally graded materials (FGM) and their fracture characteristics were evaluated (Kurd et al. 2017), protective coating (Zhang et al. 2011), CNT/rubber composites (Jiang et al. 2012), and many more. The inclusion of CNTs assisted in enhancement of mechanical, electrical, and thermal properties.

1.2.2 Graphene-Based Composite Materials

The attention towards graphene started since the isolation of graphene from bulk graphite (Novoselov et al. 2004), which then was recognized for Nobel Prize in Physics in 2010, accordingly. In that research, graphene sheets were obtained by using adhesive tape (Scotch tape) to remove flakes of graphite from a slab of highly ordered pyrolytic graphite into increasingly thinner pieces until individual atomic planes (monolayer of graphite) were gained (Randviir et al. 2014). Graphene is a one-atom-thick planar sheet of two-dimensional (2D) sheet sp^2 bonded carbon atoms that are densely packed in a honeycomb crystal lattice with remarkable properties such as high aspect ratio, large surface area, excellent electrical, thermal, mechanical properties, and so on (Dai et al. 2012; Pumera 2010; Randviir et al. 2014; Nasir et al. 2018). As the mother and components of all graphitic forms, graphene is a building block for carbon materials of all other dimensionalities, for instance 0D buckyballs, 1D nanotubes, and 3D graphite.

The preparation of graphene can be grouped into top-down and bottom-up methods. Few points such as such as cost effectiveness, scaled-up production, high electrochemical activity, conductivity, are to be considered in graphene preparation (Lv et al. 2016).

Top-down approach usually applies mechanical force or chemical intercalation to overcome the van der Waals forces between the graphene layers to achieve separation of graphene from bulk graphite, such as micromechanical cleavage (mechanical exfoliation), oxidation-exfoliation-reduction, intercalation exfoliation, solid exfoliation, and so on (Lv et al. 2016; Dong et al. 2017). In the case of mechanical exfoliation by Scotch tape, the process is less appropriate because of the low yield and lengthy process, even though the graphene produced possesses high quality (Randviir et al. 2014; Papageorgiou et al. 2015). The solvent-phase exfoliation process utilizes solvent, which can yield good quality graphene, but in quite small amount (Papageorgiou et al. 2015; Potts et al. 2011). Nevertheless, the graphene obtained through solvent-phase exfoliation is appropriate to be utilized for solution blending process in composite materials fabrication. For composite materials which needed high quantity of graphene as the filler materials, thermal exfoliation which utilizes thermal shock to obtain exfoliated graphene is considerable (Papageorgiou et al. 2015).

Bottom-up approach commonly uses a small molecule precursor to grow into graphene by CVD or chemical synthesis. For graphene prepared by CVD, they exhibit some excellent properties, due to their large crystal domains, monolayer structure and less defects in the graphene sheets, which are beneficial for boosting carrier mobility in electronic applications, and apparently in nanocomposites (Papageorgiou et al. 2015; Ke and Wang 2016). Furthermore, the layers and defects of graphene can be controlled by adjusting growth parameters such as temperature, time, catalyst, and so on.

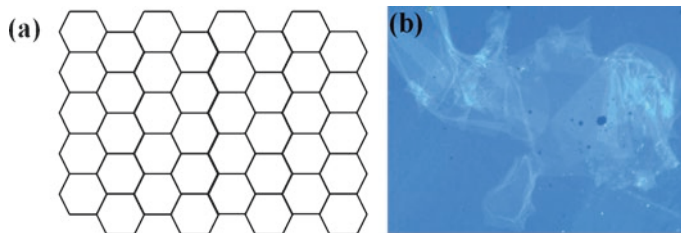


Fig. 1.2 (a) Graphene model, (b) few-layer GO on glass slide

Through the utilization of suitable physical or chemical method, production of porous graphene and doped graphene sheets can be accomplished, and high performance/functionality graphene can be further fabricated with the introduction of organic/inorganic materials. Furthermore, the production of graphene with low cost, high yield, and high quality is also a vital point. Usually, the chemical exfoliation of graphite into graphene oxides (GOs), followed by controllable reduction of GOs (with reduction agent such as hydrazine hydrate) into graphene can be considered as an efficient and low-cost method (Dong et al. 2017). Model of graphene and few-layer GO are shown in Fig. 1.2.

Similar with CNTs production, various low cost renewable carbon-based resources also can be utilized for graphene production. For instance, the growth of graphene on the surface of Cu foils under a H_2/Ar flowing atmosphere by using food, insects, and waste was reported (Ruan et al. 2011). Other materials such as paper cups, glucose, hemp, rice husk, cockroach legs, cookies, and grass also have been utilized for graphene production (Raghavan et al. 2017). Furthermore, uniform monolayer graphene film was also produced by using chicken fat oil through low pressure CVD process (Rosmi et al. 2016), and few layer graphene was also obtained from dead camphor leaves (Shams et al. 2015). Moreover, waste plastics which are rich in polyethylene and polystyrene also can be turned into high quality single crystal graphene by using ambient pressure CVD process (Sharma et al. 2014).

Graphene, derivative of graphene, and graphene hybrid materials are widely utilized in composite materials for numerous applications. For example, composite electrode with the combination of activated carbon and reduced graphene oxide (rGO) (Guardia et al. 2019), and rGO- Co_3O_4 composites (Zhang et al. 2019) exhibited enhanced supercapacitor performance. Not limited to energy storage applications, due to their excellent electrical properties, they are also used for high performance electromagnetic shielding application by using the composites consist of graphene and CNTs (Zhu et al. 2019). Graphene oxide-based composites also showed significant shape memory effect when thermally stimulated, which further reveal their potential to be utilized for actuator, biomedical device, sensor, or switches (Yan et al. 2019; Wang et al. 2019a).

1.3 Various Carbon Materials

1.3.1 Heat Treatment

Heat treatment is highly associated with pyrolysis, which is a process involves thermal decomposition of materials at certain temperature and in inert environment. Specifically, carbonization process can be further defined as a process where organic precursors are turned into carbon residues and volatile compounds during heating process in inert environment (Lin et al. 2018). Low crystalline carbon materials are usually obtained through carbonization process. At further higher temperature (>1200 °C), high crystalline carbon materials can be obtained through graphitization process (Lin et al. 2018).

Carbon materials are successfully derived from straw, corncob, and fallen leaves through carbonization at 800 °C for 0.5 h in nitrogen environment (Wu et al. 2016a). Furthermore, rice husks (RHs) are lignocellulosic materials, which is feasible to turn them into carbon materials (Wang et al. 2010). Generally, RHs are manipulated as low value energy resource, discarded, or simply burnt at the field, which will influence the air quality and threaten the environment. Through carbonization process, RHs and saw dusts can be derived into carbon materials, at 500–800 °C for 1–2 h under the presence of Argon gas (Melvin et al. 2017b; Melvin et al. 2019b). Additionally, the carbon materials produced from agro-based wastes are further utilized as activated carbon (AC) for adsorbents, electrochemical electrode composite materials, and many more. ACs can be majorly produced through chemical and physical activation, which enhanced their porosity and specific surface area. Usually, chemical activation involves mixing carbon precursor with chemical agents (KOH, H₃PO₄, H₂SO₄, K₂CO₃ etc) and the activation/carbonization takes place simultaneously when heat treated; meanwhile physical activation involves the introduction of oxidizing atmosphere (CO₂, steam, etc.) to carbonized materials (Wei and Yushin 2012). Few examples of AC utilized as adsorbents are; AC from RHs for nitrate removal from water (Satayeva et al. 2018), AC from date pits for lead ions removal (Krishnamoorthy et al. 2019), AC from pistachio wood for Pb(II) removal (Sajjadi et al. 2019). Moreover, high performance composite materials for supercapacitor electrodes are manipulated from AC derived from corn straws (Lu et al. 2017), oil palm shells (Abioye et al. 2017), etc. Interestingly, activated carbon fibers are obtained from sawdust (Huang et al. 2017), and large area activated few-layer graphene are obtained from peanut shell (Purkait et al. 2017), also for high performance supercapacitor applications.

Alternatively, ACs are also produced through microwave heating. Microwave heating, not limited to activation process, has been utilized in diverse fields due to its short time treatment and comparatively low energy consumption (Alslaibi et al. 2013). For example, carbonized saw dusts were activated through microwave heating by using K₂CO₃ (Foo and Hameed 2012). On the other hand, ACs obtained from microwave-assisted activation of petroleum coke by using KOH were used to fabricate electric double layer composite capacitors (He et al. 2010). Furthermore,

diverse types of carbon materials were also synthesized through microwave heating. Hollow carbon nanofibers were obtained from pine nut shell and palm kernel shell during microwave pyrolysis (Zhang et al. 2018; Omoriyekomwan et al. 2017). ACs which function as microwave receptor, were mixed with the biomasses during the microwave pyrolysis.

Furthermore, high crystallinity carbon materials can be obtained through heat treatment at high temperature. For instance, wrinkled few- and multi-layer graphene can be obtained from rice husks (RHs) treated at 2500 °C (Melvin et al. 2017b). Comparatively, they showed clean surface, clear edges, and relatively high crystallinity than RHs carbonized at low temperature. Composite materials consist of RHs treated at 2500 °C also exhibited significant electromagnetic wave absorption performance, over 98% absorption with thickness of 1.6 mm (Melvin et al. 2017c). Interestingly, RHs treated at 1500 °C produced a heterogeneous materials - mixture of carbon materials, silicon carbide (SiC) whiskers and SiC particles (Melvin et al. 2019c). Composite materials consist of RHs treated at 1500 °C showed over 99.9997% electromagnetic wave absorption. Furthermore, nanoparticles also can be attached onto their surface to fabricate nanocomposites (Melvin et al. 2017d). On the other hand, graphite whiskers also can be obtained when fullerene waste soot (Wang et al. 2015a), wood charcoal (Saito and Arima 2007), grounded graphite (Dong et al. 2001), and coffee grounds (Melvin et al. 2019d) are treated at various high temperatures. These graphite whiskers exhibited strong G' when investigated using Raman spectroscopy, which might be induced by the disclination of graphitized carbon layers. Vapor carbon that produced by the precursor can be assumed as the carbon source, when they are heat treated at high temperature. The high crystallinity of carbon materials obtained at high temperature might be attributed to realignment or restructure of vapor carbon. Few types of carbon materials obtained from agro-based waste materials heat treated at high temperature are shown in Fig. 1.3.

1.3.2 Plasma Enhanced Chemical Vapor Deposition (PECVD)

As mentioned above, CVD method was extensively employed for the synthesis of carbon materials including diamond, CNT, and graphene. For the sake of low-temperature synthesis of these carbon materials, plasma is involved in the CVD process, and it is regarded as plasma enhanced CVD (PECVD). In PECVD process, plasma which consists of electrons, ionized gas species (ions), and neutral species in both ground and excited states. The plasma is usually created and sustained by applying a high frequency voltage (e.g. radio frequency (rf), microwave) or direct current discharge between two electrodes to a low pressure gas. For the growth of carbon-based materials, plasma was initially utilized to fabricate diamond-like carbon (DLC) films. In 1983, Japanese researchers firstly obtained the crystalline diamond particles on silicon wafers using a gaseous mixture of H_2 and CH_4 under microwave glow discharge conditions (Kamo et al. 1983). Consequently, the

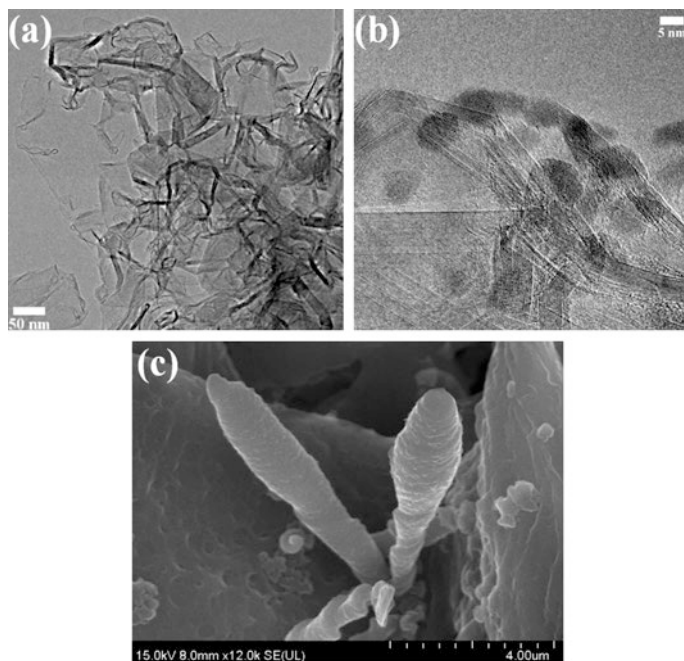


Fig. 1.3 TEM images of (a) corrugated few-layer graphene from RH treated at 2500 °C (Melvin et al. 2017b), (b) barium titanate nanoparticles immobilized onto the surface of RH treated at 2500 °C (Melvin et al. 2017d), FE-SEM image of (c) graphite whisker from waste coffee grounds treated at 2500 °C

microwave PECVD techniques with various designs have been extensively employed for diamond growth, and the resulting products with or without post treatment could be applied in the wide fields of electronic and optical devices, and electrochemical electrodes due to their excellent physical and chemical properties (Schwander and Partes 2011).

With the development of carbon materials, CNTs were firstly observed by Iijima (1991), and quickly attracted great attention in their fundamental research and applications at the beginning. The synthesis approaches of CNTs focus mainly on arc discharge, laser ablation, and CVD. In 1998, Ren et al. (1998) fabricated the CNTs on glass substrate with the decomposition of NH_3 and C_2H_2 by plasma-enhanced hot filament CVD. Compared to thermal CVD grown CNTs, the plasma-assisted CNTs not only grew at low temperatures (less than 666 °C) but also possessed vertical orientation to the substrate, thus, have a better performance in field emission emitters. The PECVD technique is most promising method, in which the decomposition and carbonization of the carbonaceous precursor have been done at low temperatures by the generation of plasma to synthesize multi- and single-walled CNTs (MWCNTs and SWCNTs). The CNT forest can be achieved even at 250–300 °C over large substrate areas under plasma condition (Kleinsorge et al. 2004; Boskovic et al. 2005), thus, they are more acceptable and applicable than

those obtained by conventional CVD. Until now, plasma grown CNTs can be used for lots of applications like energy storage and conversion, sensors, membranes, and field emission displays (Lone et al. 2017). For the application of field emission, plasma-assisted CNTs show some advantages, e.g., high electrical conductivity and low threshold field. However, there is a stable problem that the tallest CNT in the forest experiences the highest field and emits the entire current, which leads to burn it out (Zanin et al. 2013). Thus, some attempts have been employed to overcome it, e.g. combining CNTs with other materials to form composites. For example, the CNTs decorated with Er NPs (Shrestha et al. 2010), ZnO NPs (Ho et al. 2008), and nanodiamond (Guglielmotti et al. 2009) demonstrated the improved emission properties. Zanin et al. (2013) reported the vertically-aligned CNT (VACNT) and DLC composite (Fig. 1.4), in which they were synthesized in the system of $N_2-H_2-CH_4$ and $C_6H_{14}-Ar$ using different PECVD techniques, respectively, like a honeycomb structure with significant enhancement in emission current, lifetime, stability, and flickering features. Due to higher conductivity and faster diffusion, the VACNTs on the metal substrates were more suitable as the electrodes of electrochemical devices,

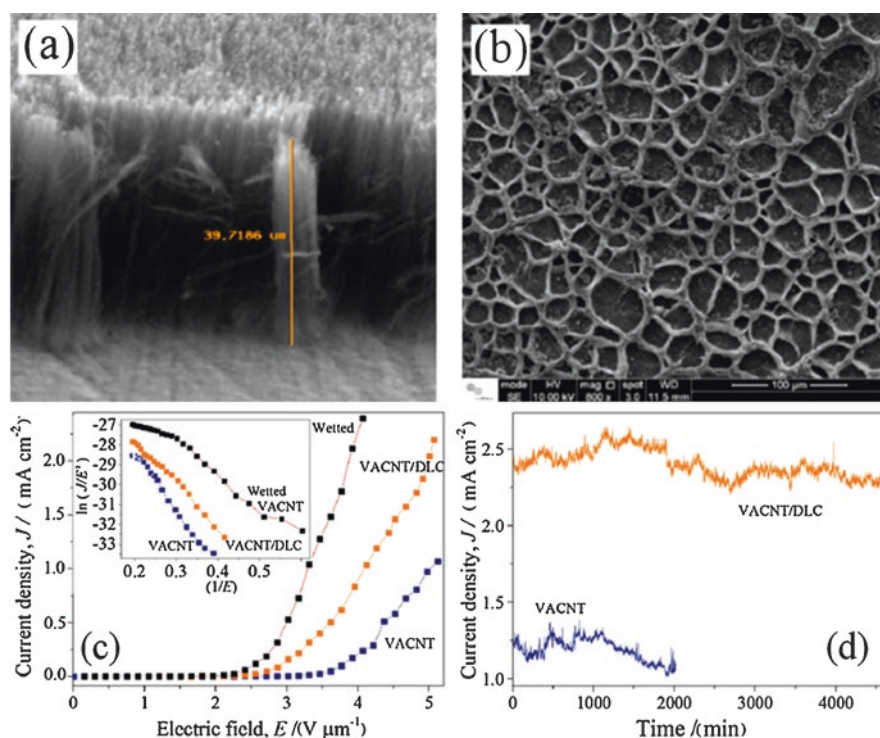


Fig. 1.4 SEM images of the VACNT films (a) without and (b) with the DLC coating, (c) Field-emission characteristics of the VACNT film, the DLC/VACNT film, and the wetted VACNT film. Inset: The corresponding Fowler-Nordheim plots from the three types of samples. (d) Field emission current-density stability test from the VACNT films with and without the DLC coating (Zanin et al. 2013)

e.g. supercapacitors and lithium ion batteries (LIBs), in comparison with the free-standing CNTs. The VACNTs composites can further improve the properties of LIBs and supercapacitors (Amade et al. 2011; Saghafi et al. 2014; Malik et al. 2017; Jiang et al. 2019).

Similar to CNTs, graphene-based materials can be also synthesized by various PECVD techniques since the first isolation of graphene using adhesive tape method (Nandamuri et al. 2010; Kim et al. 2011a; Kim et al. 2011b; Bo et al. 2013). In these plasma reactors, the carbonaceous gas was usually decomposed into carbon radicals to eventually form graphene materials on the substrate with the help of H_2 and/or Ar (other gases) as etching reagent. Among those graphene-based materials synthesized by PECVD, vertical graphene (VG), which grew perpendicularly to the substrate (Wang et al. 2011a), has demonstrated some unique characteristics (Fig. 1.5), e.g., nonagglomerated porous internetworked morphology, an abundant of open and sharp edges, and controllable structures. Thus, it makes VG possess more interesting properties, e.g., high electrical conductivity, high surface area, and high electrochemical activity, and many promising applications, e.g., field emission emitters, biosensors, catalysts or catalysts supports, and electrodes of electrochemical devices (Wang et al. 2011b, 2012a, 2012b). In addition, the VG films can be more easily formed on the different substrates including metals, semiconductors, and insulators with any shapes or sizes. It makes VG growth look like substrate-independent process that it attributes to the requirement of no catalyst and easy formation of nucleation sites under plasma conditions. Chen group utilized an atmospheric pressure PECVD to decompose CH_4 on the surface of the CNTs to form hybrid graphene-CNT composites, which have potential electronic and optoelectronic applications (Yu et al. 2011). More interestingly, the VG structures can be achieved from not only the carbonaceous gases but also liquid or solid precursors, including *Melaleuca alternifolia*, milk, honey, butter, sugar, cheese, solid carbon, and polymer (Seo et al. 2013a, 2013b, Wang et al. 2014a, 2014b, Jacob et al. 2015) under various plasma conditions though the resulting VG films exhibited different morphology and microstructure, as partially shown in Fig. 1.5.

The waste plant biomass, which was usually utilized as a source for activated carbon, has extensively been employed to synthesize other novel carbon structures including CNTs, graphene, and their derivatives (Wang et al. 2015b, 2015c), as

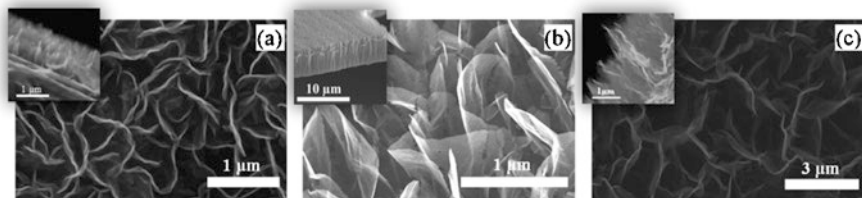


Fig. 1.5 Morphological structures of the VG films from different precursors: (a) CH_4 (Wang et al. 2011a), (b) Kapton polyimide (Wang et al. 2014a), (c) solid carbon (Wang et al. 2014b). Inset: the corresponding cross-sectional images

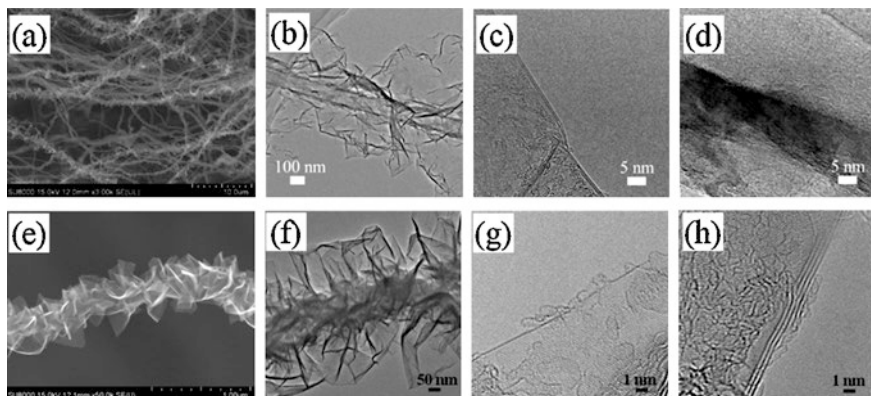


Fig. 1.6 Morphologies and microstructures of the g-CNTs and the GSF synthesized from RHs and coffee grounds, respectively, by microwave plasma irradiation technique: (a) SEM, and (b–d) TEM images of the g-CNTs, (e) SEM, and (f–h) TEM images of the GSF. (Wang et al. 2015b, 2015c)

depicted in Fig. 1.6. Microwave plasma irradiation technique was utilized to treat RHs, which located in the home-made Ni box, and found the graphene-CNT hybrid structures, in which graphene sheets grew on the walls of CNTs (named as graphenated CNTs, g-CNTs), on the Ni surface. The g-CNTs exhibited more excellent electrochemical properties than individual CNTs and graphene in the application of supercapacitors. In 2015, graphene-sheet fiber (GSF) were firstly synthesized when the coffee ground powders replaced the RHs. Differ from the g-CNTs, GSF consists of only graphene sheets without the CNT structure inside. The resulting GSFs have relatively excellent electrical conductivity and fantastic specific capacitance.

1.3.3 Hydrothermal Treatment

An aqueous solution of organic substances such as saccharides (glucose, sucrose or starch) or compounds (e.g., furfural) which was heat-treated at a range of temperatures of 150–350 °C for a certain time, the products including water-soluble organic substances and insoluble carbon-rich solids will be formed (Sevilla and Fuertes 2009a). The process, termed as hydrothermal carbonization (HTC), has attracted great interest in recent years. As was known, the HTC is not a new process, and has been utilized to treat various saccharides to investigate the mechanism information of natural coalification during the first decades of last century (Sevilla and Fuertes 2009a). Subsequently, the HTC of the cellulose was studied to obtain liquid chemicals or other solid products, which have the same composition of those obtained from the HTC of the glucose, suggesting that the hydrolysis products for both substances are similar (Van Krevelen 1950).

Wang et al. (2001) first reported the hydrothermal treatment of sucrose to produce carbon microspheres. Subsequently, Sun and Li (2004a) obtained similar

carbon spheres (CSs) by the HTC of the glucose, in which their sizes were adjustable through the experimental parameters and they can be loaded with metal NPs to form the hybrid carbon/metal materials (e.g., C/Ag, C/Cu, C/Au, C/Pd, C/Te). Studies have shown that the HTC-assisted CSs can be employed as sacrificial templates for fabricating hollow spherical structures of inorganic compounds (e.g., Ga₂O₃, GaN, WO₃, SnO₂) (Sun and Li 2004b; Li et al. 2004; Wang et al. 2007). The CSs synthesized from the HTC of different saccharides (glucose, sucrose or starch) can be used as precursors for the production of graphitic carbon nanocoils (Fig. 1.7(c)-(d)) with the help of Ni under nitrogen up to 900 °C for 3 h, and the products supported PtRu NPs for metal electrooxidation (Sevilla et al. 2007). Significantly, the glucose-derived CSs (Fig. 1.7(a)-(b)) were graphitized at extremely high temperatures in the range of 1200-2900 °C to achieve discrete fragments of curved graphitic planes (Wang et al. 2017), which are similar to heat-treated glassy carbon. But, they were different from the tetrahydrofuran-derived pyrolytic spheres (Zhang et al. 2006) and the hydrocarbon-derived carbon spheres by CVD technique (Wang et al. 2005) at extremely high temperatures, which demonstrated concentric polyhedral graphitic shells. It implied that the microstructures of the resulting CSs after high temperature treatment were strongly dependent of the precursors.

Besides the saccharides (glucose, sucrose or starch), the cellulose can be converted into carbon microspheres (2–5 μm) by the HTC process at the temperatures in the range of 220–250 °C (Sevilla and Fuertes 2009b). The results confirmed that the formation of CSs involved into the path of a dehydration process, similar to the previous observation for the hydrothermal transformation of saccharides. Biomass is a biological matter that incorporates all living matter on earth, and mainly consists of cellulose, hemicellulose, and lignin. Thus, biomass is suitable substance for the formation hydrochar under HTC, which strongly depend on the process parameters including temperature, feed type, residence time, pressure, and catalyst (Nizamuddin et al. 2017).

In addition, hollow CSs with controllable size and morphology have been developed by the HTC of α-cyclodextrin in the presence of Pluronic F127 as a soft template (Yang et al. 2013), as illustrated in Fig. 1.7(e) and (f). Uniform carbon nanofibers (about 50 nm in diameter and some micrometers in length) with high aspect ratio could be produced using the HTC of the glucose in the present of Te nanowires (Qian et al. 2006), as shown in Fig. 1.7(g) and (h). The pure carbon nanofibers can be obtained by removal of the core of the product by treatment of with a mix aqueous solution of HCl and H₂O₂ at RT for 12 h.

HTC of biomass such as glucose and cellulose typically produces CSs with the diameter in micrometer size, which are insulating. When adding a certain amount of graphene oxide (GO) to glucose, the HTC products exhibit significant change in their morphologies and improve the conductivity of carbon materials with high degree of carbonization. At low mass loading of GO, HTC treatment can lead to dispersed carbon platelets with tens of nanometers in thickness, while at high mass loading, free-standing carbon monoliths can be obtained (Krishnan et al. 2014). GO, a two-dimensional single atomic sheet, is the chemical exfoliation product of graphite powders, and has rich oxygen-containing functional groups, e.g., epoxy

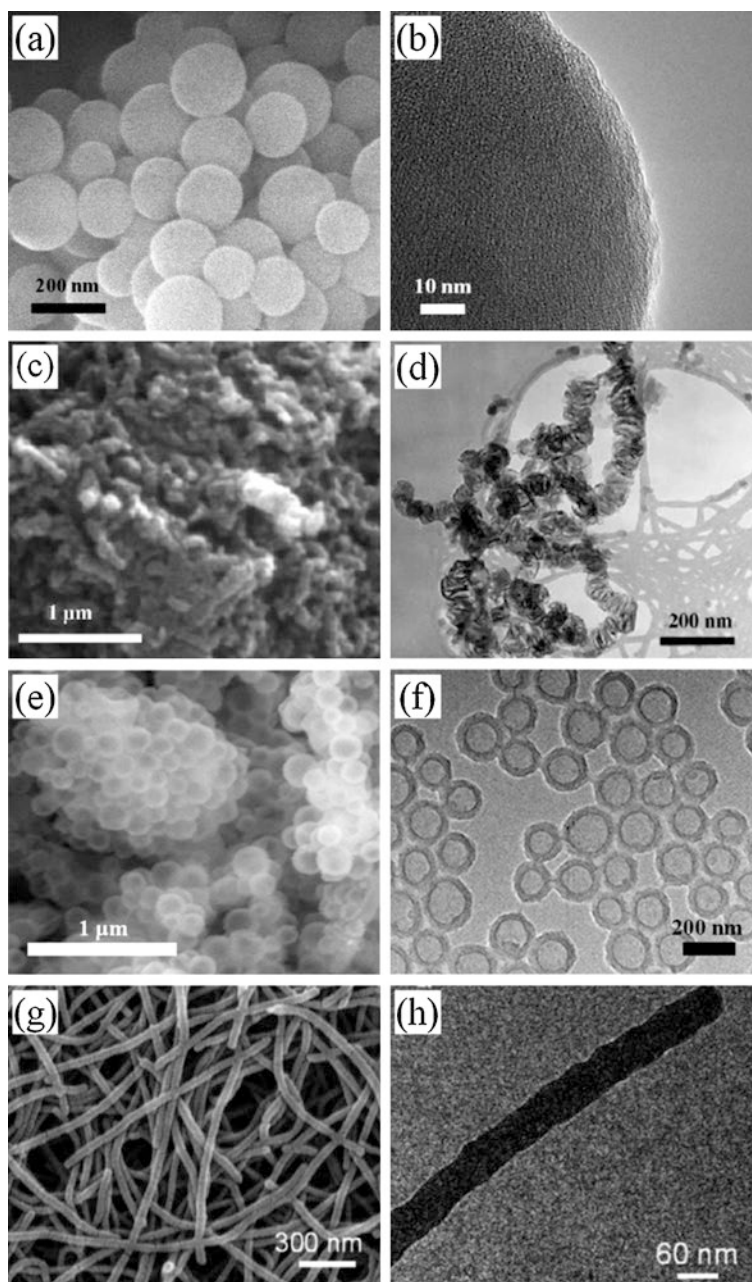


Fig. 1.7 SEM and TEM images of (a-b) glucose-derived carbon spheres (Wang et al. 2017), (c-d) saccharide-derived graphitic carbon nanocoils (Sevilla et al. 2007), (e-f) α -cyclodextrin-derived hollow carbon spheres (Yang et al. 2013), (g-h) glucose-derived carbon nanofibers under HTC conditions (Qian et al. 2006)

and hydroxyl groups, decorating the segregated nanographitic domains on their basal planes so that it is easily dispersed in water and many polar solvents. Compared with original GO sheets, reduced GO (rGO) sheets demonstrate the more outstanding physiochemical properties and promising applications. Thus, various attempts, e.g., chemical, thermal, solvothermal, and hydrothermal reductions (Zhou et al. 2009; Zhao et al. 2012; Huang et al. 2018), have been employed to reduce GO sheets into rGO sheets. Among them, hydrothermal reduction of GO is a simple, fast, and environmentally friendly route which involves water only without adding any toxic reducing agents. The graphene aerogel can be obtained from rGO using hydrothermal process, and demonstrated excellent elastic modulus, good electrical conductivity, high specific capacity, and thermal stability. The results confirmed that the properties of graphene aerogels strongly depend on GO concentration and hydrothermal reaction time (Xu et al. 2010). In order to achieve wider applications, graphene-containing composite materials have been extensively investigated. Researchers utilized one-step hydrothermal method to synthesize graphene-based composites, such as TiO_2 -rGO, Co_3O_4 -rGO, and doped rGO (Shen et al. 2011; Liu et al. 2013; Zhang et al. 2017), in which exhibited the improved properties and performances in supercapacitors and batteries.

During the HTC process, the GO as a template and catalyst can promote the polymerization of the fragments decomposed from egg proteins to form egg protein-derived carbon/rGO composite for supercapacitor electrode with high specific capacitance, good rate capability and excellent cycling stability (Ma et al. 2017). Hydrothermal approach was also employed to cut the thermally rGO sheets into surface-functionalized graphene quantum dots (GQDs) with 9.6 nm average diameter (Pan et al. 2010). The resulting GQDs exhibited bright blue photoluminescence due to their large edge effect.

1.3.4 Electro-Deposition Using Molten Salts

Over the course of years, the rapid growth of industrial sectors, the increase in human population, and open agricultural burning give rise to carbon dioxide gas emission into the atmosphere. The atmospheric concentration of carbon dioxide gas had reached an alarming level. According to National Oceanic and Atmospheric Administration (NOAA) and the American Meteorological Society report released in August 2018 entitled State of the Climate in 2017, the global atmospheric carbon dioxide concentration for the year 2017 was at 405.0 ± 0.1 ppm. The effort in reducing the level of carbon dioxide gas in the atmosphere had been one of the great concerns in this modern world. The awareness of the climate change gives way to researchers in utilizing carbon dioxide as the source of conversion to value-added product, therefore carbon capture and utilization (CCU) technologies (Alper and Yuksel Orhan 2017; Stuardi et al. 2019; Styring et al. 2011; Yan and Zhang 2019) was extensively studied either in industry or academically (Yuan et al. 2016). The conversion of carbon dioxide gas introduce the end products which contains the

carbon from the gas as a result of physical and chemical processes (Song 2002). Electrochemical conversion of carbon dioxide gas in molten salt electrolyte as one of the utilization method had progress rapidly due to the molten salt exceptional properties, for instance low vapor pressure, high electronic conductivity and low cost (Ge et al. 2016).

Electrolytic generated carbon in electrolysis of molten salts was accidentally discovered in the early 1900's where Haber and Bruner (1904) attained significant carbon deposition from barium chloride and barium carbonate mixture at 580 °C. While in the 1940's, Andrieux and Weiss (1944) unintentionally found carbon by utilizing carbonates and halides mixtures to synthesis inorganic carbides at 750 °C via electrochemical route. In 1960's, inspired by the previous accidental findings; Ingram et al. (1966) studied the occurrence of carbon deposition in electrolysis of molten carbonates with argon and carbon dioxide atmosphere, its characteristics and the properties of the deposited carbon, however limited interest was shown in this study throughout the years. Recently, researchers show interest in the electro-deposition of solid carbon using molten salts electrolyte with continuous supply of carbon dioxide gas. It is due to the discoveries of wide variation of interesting carbon microstructure and the utilization of carbon dioxide gas as carbonate source in the molten salt electrolysis process (Deng et al. 2018; Dimitrov et al. 2002; Gakim et al. 2015; Ge et al. 2016; Ijije et al. 2014a; Ingram et al. 1966; Karen et al. 2018; Le Van et al. 2009; Novoselova et al. 2008; Tang et al. 2013; Yin et al. 2013).

Wide variety of carbonaceous materials were discovered from electrolysis of molten salt electrolytes. The carbonaceous materials sizes ranging from micro- to nano- and was found to exhibit diverse microstructures depending on the electrolysis process parameters, *i.e.* electrolytes, substrates, temperatures, current densities and deposition potentials (Hughes et al. 2015; Kawamura and Ito 2000). There were various reasons and factors on the parameter selection, however some of the studies targeted selective electrolyte and electrode type due to the desired end product *i.e.* in the synthesis of carbon nanotubes or nanomaterials by using molten chloride salt. Molten chloride salt (LiCl, NaCl, KCl, and more) was utilized alongside graphite electrodes with carbon nanotubes as main product (Chen et al. 1998; Hsu et al. 1996). While Kamali et al. (2011) study the use of different type of graphite electrode to the carbon nanomaterial obtained by using LiCl electrolyte, further study by Kamali and Fray (2013) look into the corrosion of the electrode in mixture of LiCl salt with graphite powder. However, the selection of electrolyte should be considered carefully which could produce carbon materials as the end product. The molten salt electrolyte should be able to dissolve the O^{2-} ion which the ion is a product of carbon deposition and able to absorb CO_2 gas and convert it to CO_3^{2-} ions (Ijije et al. 2014b). Another important factor for successful carbon deposition is the presence of Li^+ ions in the electrolyte (Ingram et al. 1966; Delimarskii et al. 1968; Kawamura and Ito 2000; Massot et al. 2002; Ijije et al. 2014b). Based on the study on the role and effect of the alkali metal ions in electrolysis process, notable Na^+ , K^+ and Li^+ ions, Ijije and Chen (2016) found that electrolyte containing Li^+ ion (Li_2CO_3) produced carbon material while electrolyte containing Na^+ (Na_2CO_3) and K^+

(K_2CO_3) produced alkali metal as the main cathodic reaction. Over the years, the selection of electrodes in the electrolysis process was not carefully explain by researchers, nonetheless, the use of silver, nickel, gold, tungsten, platinum or copper as electrodes have been reported (Ingram et al. 1966; Lantelme et al. 1999; Le Van et al. 2009; Tang et al. 2013; Yin et al. 2013; Ge et al. 2016; Deng et al. 2018). Likewise, the temperature, current densities and deposition potentials selection for the process were not vastly studied and limited information was available. Though, the process temperature often chosen while considering the melting temperature of the selected electrolyte.

Interesting microstructures was observed in the carbon materials obtained either in single-salt electrolyte of mixture of two or more salt. The electrolysis of single Li_2CO_3 yields micro-sized irregular shaped flakes under process temperature of 740 °C and voltage supply of 4 V by using stainless steel electrodes (Ijije and Chen 2016). Whereas nano-sized carbon nanofibers was produced under 730 °C with coiled galvanized steel wire cathode and Ni anode (Ren et al. 2015), and carbon nanotubes was observed in Wu et al. (2016b) study under the temperature of 770 °C and Ni as cathode with addition of ZnO additive (1 wt%). Figure 1.8 shows the findings of the studies respectively.

Diverse microstructures were observed in mixture of two or more salt electrolyte. Dimitrov (2009) observed nano-balls and flower-like sheets in electrolysis of binary $LiCl-Li_2CO_3$ using graphite electrodes at 700 °C, whereas Ge et al. (2015) found quasi-spherical microstructures with inert platinum anode and tungsten cathode at 700 °C of electrolysis temperature. On the other hand, Deng et al. (2018) obtained wide variety of carbon microstructures with the addition of salt additive ($CaCO_3$) into the binary $LiCl-KCl$. Crater-like, nanofibers, coral, quasi-spherical, spherical, carbon sheets, shell-like structure, flakes and aggregated nanoparticles was found in the study. While Kawamura and Ito (2000) and Song et al. (2012) observed aggregated quasi-spherical structure in electrolysis of ternary $LiCl-KCl-K_2CO_3$, at 450 °C with rectangular sheet of aluminum as cathode and glassy carbon

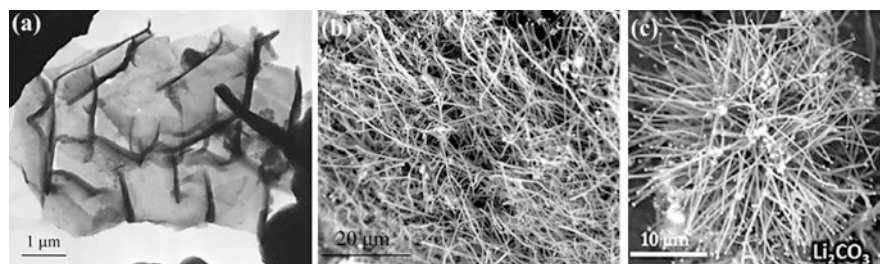


Fig. 1.8 The findings of carbon microstructures deposited in single Li_2CO_3 electrolyte, (a) TEM image of carbon deposited under 740 °C with 4 V in CO_2 atmosphere (Ijije and Chen 2016), (b) SEM image of nano-sized carbon nanofibers produced under 730 °C with coiled galvanized steel wire cathode and Ni anode (Ren et al. 2015), and (c) SEM image of carbon nanotubes obtained under the temperature of 770 °C and Ni as cathode with addition of 1 wt% ZnO additive (Wu et al. 2016b)

rod anode, and at 500 °C with graphite electrodes, respectively. Ternary mixture of $\text{Li}_2\text{CO}_3\text{-Na}_2\text{CO}_3\text{-K}_2\text{CO}_3$ was widely use as electrolyte since Ingram et al. (1966) successfully obtained carbon deposition. Groult et al. (2006) found nano-sized carbon particles in electrolysis of the ternary electrolyte at 450 °C with gold-sheet anode and Ni-sheet cathode, whereas Le Van et al. (2009) discover nano-sized quasi-spherical carbon with graphite anode and Ni cathode. While Yin et al. (2013) observed aggregated nano-sized carbon particles and flakes with SnO_2 rod anode and Ni-sheet cathode at 500 °C, Tang et al. (2013) obtained micro- and nano-sized flakes, nanowires, particles and thin sheets by using SnO_2 rod anode and U-shape Ni sheet cathode at process temperature of 450, 550, and 650 °C. Gakim et al. (2015) found micro-sized aggregated grape-like structure in electrolysis of $\text{CaCO}_3\text{-CaCl}_2\text{-KCl-LiCl}$ quaternary mixture at temperature range between 575 and 585 °C. Study by Karen et al. (2018) in electrolysis of newly formulated ternary $\text{CaCO}_3\text{-Li}_2\text{CO}_3\text{-LiCl}$ salt mixture at 550–650 °C and 4 – 6 V cell voltage using stainless steel as electrodes with CO_2 atmosphere showed five dominant microstructures: grape-like, tubes, thread-like, spheres, and flakes under the SEM analysis, as shown in Fig. 1.9(a) - (e) respectively.

Electrolysis involves the splitting of a particular substance when electrical energy was introduced into the system, and it is frequently applied to decompose a compound to its elements. The electrolyte in the electrolysis process could be the pure compound, for example H_2O or a molten salt, or a mixture of two or more molten salts (Silberberg 2006). The utilization of carbon dioxide gas as carbon source in the electrolysis of molten salt electrolyte produces carbonaceous materials.

Electro-deposition of solid carbon via electrolysis of molten salt in CO_2 atmosphere can be carried out in an electrolytic cell. The cell requires an electrolyte

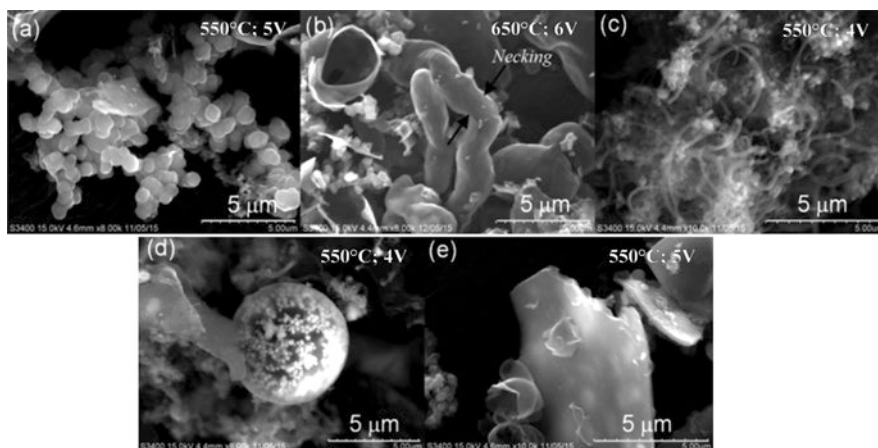
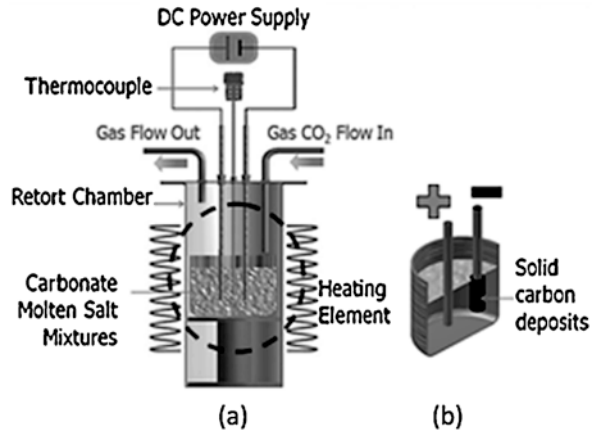


Fig. 1.9 The example of SEM images for (a) grape-like, (b) tubes, (c) thread-like, (d) sphere, and (e) flakes, as dominant microstructures found in the deposited solid carbon prepared at 550 and 650 °C with voltage supply of 4 – 6 V using ternary $\text{CaCO}_3\text{-Li}_2\text{CO}_3\text{-LiCl}$ salt mixture (Karen et al., 2018)

Fig. 1.10 The schematic diagram (not according to scale) of (a) experimental set-up for the electro-deposition of solid carbon via electrolysis process and (b) solid deposition on cathode surface for electrolysis in CO₂ gas environment (Karen et al. 2018)



which contains ions (cations and anions) and able to conduct electric when it is in liquid form. Electric current can be supplied to the electrolyte by the positive and negative electrodes which immersed in the electrolyte. CO₂ gas can be flowed into the system to replenish the carbonate ions (CO_3^{2-} as carbon source) in the electrolyte for continuous carbon deposition on the cathode surface. Fig. 1.10 displayed the example of experimental setup for electrolysis process and the deposition of solid carbon the cathode surface based on Karen et al. (2018) study.

The deposition of carbon occurred on the surface of cathode electrode as a result of the conversion reaction happened at the interface of cathode and the electrolyte (Ingram et al. 1966), as soon as the voltage was supplied to the system. The carbon source, carbonate ions (CO_3^{2-}), will be reduced to carbon in the electrolysis process in two steps of reaction as stated below (Ingram et al. 1966; Kawamura and Ito 2000; Kaplan et al. 2002; Massot et al. 2002; Le Van et al. 2009; Ijije et al. 2014c; Gakim et al. 2015).

Step 1:	$CO_3^{2-} + 4e^- \rightarrow C (s) + 3O^{2-}$	(1)
	$CO_3^{2-} + 2e^- \rightarrow CO_2^{2-} + O^{2-}$ then $CO_2^{2-} + 2e^- \rightarrow C (s) + 2O^{2-}$	(2 & 3)
Step 2:	$O^{2-} + CO_2 (g) \rightleftharpoons CO_3^{2-}$	(4)

The CO_3^{2-} ions first reduced to carbon either by the single-step process based on reaction (1) (Ingram et al. 1966; Kaplan et al. 2002; Massot et al. 2002), or the two-step process based on reaction (2) and (3) (Delimarskii et al. 1968; Ito et al. 1992). Later, the molten salt electrolyte absorbs the CO₂ gas through reaction (4), and regenerates CO_3^{2-} ions in the electrolyte. The reactions cycle enables the continuous production of carbon on the cathode surface.

The application of carbon produced by electrolysis of molten salt electrolyte is not vastly studied. However, it has the potential to be utilized in various spectrum as the carbon obtained from the process exhibits a diverse microstructures and particle

sizes ranging from micro to nano sizes. For instance, composite materials for energy storage electrode (Ijje et al. 2014c). Moreover, the carbon could be further treated for attachment of desirable functional groups, *i.e.* carboxyl and hydroxyl groups, on the carbon surface which improved its dispersion ability, and later can be utilized as carbon filler in fabrication of composites or attachment of other particles onto their surface in fabrication of hybrid composites. Carbon fillers, *i.e.* carbon nanotubes (Anagappan et al. 2013), carbon nanofibers and carbon black, can be used as composites filler, and when mixing the carbon fillers with polymers, it could improve the overall mechanical, electrical and thermal stability.

1.4 Conclusions

In this chapter, carbon materials from various sources for composite materials are mainly described. Obviously, by using different material sources and methods, a great variety of carbon materials can be produced, such as carbon nanotube, graphene, carbon sphere, carbon flake, graphite whisker, and many more. Furthermore, the carbon materials also can be integrated with other materials, in order to achieve higher performance or specifically targeted properties. The carbon materials can be utilized for composite materials in vast fields and applications, such as energy storage devices, actuator, shape memory material, electromagnetic wave absorber, functionally graded material, and many more. Carbon-based composite materials is a prominent candidate to tackle our current or future demands to satisfy various necessities.

Acknowledgement This work was supported by Universiti Malaysia Sabah (Grant number GUG0386-2/2019), Malaysia.

References

- Abioye AM, Noorden ZA, Ani FN (2017) Synthesis and characterizations of electroless oil palm shell based-activated carbon/nickel oxide nanocomposite electrodes for supercapacitor applications. *Electrochim Acta* 225:493–502. <https://doi.org/10.1016/j.electacta.2016.12.101>
- Ajayan PM, Stephan O, Colliex C, Trauth D (1994) Aligned carbon nanotube arrays formed by cutting a polymer resin - nanotube composite. *Science* 265(5176):1212–1214. <https://doi.org/10.1126/science.265.5176.1212>
- Ali M, Hirai T (2011) Characteristics of the creep-induced bending deformation of a PVC gel actuator by an electric field. *J Mater Sci* 46(24):7681–7688. <https://doi.org/10.1007/s10853-011-5746-7>
- Alper E, Yuksel Orhan O (2017) CO₂ utilization: developments in conversion processes. *Petroleum* 3(1):109–126. <https://doi.org/10.1016/j.petlm.2016.11.003>
- Alslaibi TM, Abustan I, Ahmad MA, Foul AA (2013) A review: production of activated carbon from agricultural byproducts via conventional and microwave heating. *J Chem Technol Biotechnol* 88(7):1183–1190. <https://doi.org/10.1002/jctb.4028>

- Amade R, Jover E, Caglar B, Mutlu T, Bertran E (2011) Optimization of MnO₂/vertically aligned carbon nanotube composite for supercapacitor application. *J Power Source* 196(1):5779–5783. <https://doi.org/10.1016/j.jpowsour.2011.02.029>
- Anagappan S, Thirumal V, Ramkumar K, Visuvasam A (2013) Synthesis of carbon nanotubes by molten salt technique. *Chem Sci Trans* 2(2):575–583. <https://doi.org/10.7598/cst2013.394>
- Andrieux L, Weiss G (1944) Productions of electrolysis of molten salts with an iron anode. *Comptes Rendu* 217:615
- Araga R, Sharma CS (2017) One step direct synthesis of multiwalled carbon nanotubes from coconut shell derived charcoal. *Mater Lett* 188:205–207. <https://doi.org/10.1016/j.matlet.2016.11.014>
- Bazargan A, McKay G (2012) A review – synthesis of carbon nanotubes from plastic wastes. *Chem Eng J* 195–196:377–391. <https://doi.org/10.1016/j.cej.2012.03.077>
- Bi C, Zhu M, Zhang Q, Li Y, Wang H (2011) Synthesis and electromagnetic wave absorption properties of multi-walled carbon nanotubes decorated by BaTiO₃ nanoparticles. *J Nanosci Nanotechnol* 11(2):1030–1036. <https://doi.org/10.1166/jnn.2011.3046>
- Bo Z, Yang Y, Chen J, Yu K, Yan J, Cen K (2013) Plasma-enhanced chemical vapor deposition synthesis of vertically oriented graphene nanosheets. *Nanoscale* 5:5180–5204. <https://doi.org/10.1039/c3nr33449j>
- Boskovic BO, Golovko VB, Cantoro M, Kleinsorge B, Chuang AH, Ducati C, Hofmann S, Robertson J, Johnson BFG (2005) Low temperature synthesis of carbon nanofibres on carbon fibre matrices. *Carbon* 43:2643–2648. <https://doi.org/10.1016/j.carbon.2005.04.034>
- Chen GZ, Fan X, Luget A, Shaffer MS, Fray DJ, Windle AH (1998) Electrolytic conversion of graphite to carbon nanotubes in fused salts. *J Electroanal Chem* 446(1–2):1–6. [https://doi.org/10.1016/S0022-0728\(97\)00552-4](https://doi.org/10.1016/S0022-0728(97)00552-4)
- Dai L, Chang DW, Baek JB, Lu W (2012) Carbon nanomaterials for advanced energy conversion and storage. *Small* 8(8):1130–1166. <https://doi.org/10.1002/sml.201101594>
- Delimarskii YK, Shapoval VI, Grishchenko VF, Vasilenko VA (1968) Peculiarities of the cathodic liberation of carbon in the electrolysis of molten carbonates. *Dokl Akad Nauk SSSR* 183(6):1332–1334
- Deng B, Tang J, Gao M, Mao X, Zhu H, Xiao W, Wang D (2018) Electrolytic synthesis of carbon from the captured CO₂ in molten LiCl–KCl–CaCO₃: critical roles of electrode potential and temperature for hollow structure and lithium storage performance. *Electrochim Acta* 259:975–985. <https://doi.org/10.1016/j.electacta.2017.11.025>
- Dimitrov AT, Chen GZ, Kinloch IA, Fray DJ (2002) A feasibility study of scaling-up the electrolytic production of carbon nanotubes in molten salts. *Electrochim Acta* 48(1):91–102. [https://doi.org/10.1016/S0013-4686\(02\)00595-9](https://doi.org/10.1016/S0013-4686(02)00595-9)
- Dimitrov AT (2009) Study of molten Li₂CO₃ electrolysis as a method for production of carbon nanotubes. *Maced J Chem Chem Eng* 28(1):111–118. <https://doi.org/10.20450/mjcc.2009.226>
- Dong J, Shen W, Zhang B, Liu X, Kang F, Gu J, Li D, Chen N (2001) New origin of spirals and new growth process of carbon whiskers. *Carbon* 39(15):2325–2333. [https://doi.org/10.1016/S0008-6223\(01\)00064-1](https://doi.org/10.1016/S0008-6223(01)00064-1)
- Dong Y, Wu ZS, Ren W, Cheng HM, Bao X (2017) Graphene: a promising 2D material for electrochemical energy storage. *Sci Bull* 62(10):724–740. <https://doi.org/10.1016/j.scib.2017.04.010>
- Dong Y, Xia H, Zhu Y, Ni QQ, Fu Y (2015) Effect of epoxy-graft-polyoxyethylene octyl phenyl ether on preparation, mechanical properties and triple-shape memory effect of carbon nanotube/water-borne epoxy nanocomposites. *Compos Sci Technol* 120:17–25. <https://doi.org/10.1016/j.compscitech.2015.09.011>
- Foo KY, Hameed BH (2012) Mesoporous activated carbon from wood sawdust by K₂CO₃ activation using microwave heating. *Bioresour Technol* 111:425–432. <https://doi.org/10.1016/j.biortech.2012.01.141>
- Gakim M, Khong LM, Janaun J, Liew WYH, Siambun NJ (2015) Production of carbon via electrochemical conversion of CO₂ in carbonates based molten salt. *Adv Mater Res* 1115:361–365. <https://doi.org/10.4028/www.scientific.net/AMR.1115.361>

- Ge J, Hu L, Wang W, Jiao H, Jiao S (2015) Electrochemical conversion of CO₂ into negative electrode materials for Li-ion batteries. *ChemElectroChem* 2(2):224–230. <https://doi.org/10.1002/celec.201402297>
- Ge J, Wang S, Hu L, Zhu J, Jiao S (2016) Electrochemical deposition of carbon in LiCl-NaCl-Na₂CO₃ melts. *Carbon* 98:649–657. <https://doi.org/10.1016/j.carbon.2015.11.065>
- Groult H, Kaplan B, Lantelme F, Komaba S, Kumagai N, Yashiro H, Nakajima T, Simon B, Barhoun A (2006) Preparation of carbon nanoparticles from electrolysis of molten carbonates and use as anode materials in lithium-ion batteries. *Solid State Ionics* 177(9–10):869–875. <https://doi.org/10.1016/j.ssi.2006.01.051>
- Guardia L, Suárez L, Querejeta N, Vretenár V, Kotrusz P, Skákalová V, Centeno TA (2019) Biomass waste-carbon/reduced graphene oxide composite electrodes for enhanced supercapacitors. *Electrochim Acta* 298:910–917. <https://doi.org/10.1016/j.electacta.2018.12.160>
- Guglielmotti V, Chieppa S, Orlanducci S, Tamburri E, Toschi F, Terranova ML, Rossi M (2009) Carbon nanotube/nanodiamond structures: an innovative concept for stable and ready-to-start electron emitters. *Appl Phys Lett* 95:222113. <https://doi.org/10.1063/1.3269929>
- Haber F, Bruner L (1904) Das Kohlenelement, eine Knallgaskette. *Z Elektrochem Angew Phys Chem* 10(37):697–713. <https://doi.org/10.1002/bbpc.19040103702>
- He X, Geng Y, Qiu J, Zheng M, Long S, Zhang X (2010) Effect of activation time on the properties of activated carbons prepared by microwave-assisted activation for electric double layer capacitors. *Carbon* 48(5):1662–1669. <https://doi.org/10.1016/j.carbon.2010.01.016>
- Hierold C, Brand O, Fedder GK, Korvink JG, Tabata O (2008) Carbon nanotube devices: properties, modeling, integration and applications, vol 8. Wiley, Chichester
- Ho YM, Yang GM, Zheng WT, Wang X, Tian HW, Xu Q, Li HB, Liu JW, Qi JL, Jiang Q (2008) Synthesis and field electron emission properties of hybrid carbon nanotubes and nanoparticles. *Nanotechnology* 19(6):065710. <https://doi.org/10.1088/0957-4484/19/6/065710>
- Hsu WK, Terrones M, Hare JP, Terrones H, Kroto HW, Walton DRM (1996) Electrolytic formation of carbon nanostructures. *Chem Phys Lett* 262(1–2):161–166. [https://doi.org/10.1016/0009-2614\(96\)01041-X](https://doi.org/10.1016/0009-2614(96)01041-X)
- Huang H-H, De Silva K, Kumara GRA, Yoshimura M (2018) Structural evolution of hydrothermally derived reduced graphene oxide. *Sci Rep* 8:6849. <https://doi.org/10.1038/s41598-018-25194-1>
- Huang X, Chen Z, Tong L, Feng M, Pu Z, Liu X (2013) Preparation and microwave absorption properties of BaTiO₃@MWCNTs core/shell heterostructure. *Mater Lett* 111:24–27. <https://doi.org/10.1016/j.matlet.2013.08.034>
- Huang Y, Liu Y, Zhao G, Chen JY (2017) Sustainable activated carbon fiber from sawdust by reactivation for high-performance supercapacitors. *J Mater Sci* 52(1):478–488. <https://doi.org/10.1007/s10853-016-0347-0>
- Hu H, Onyebueke L, Abatan A (2010a) Characterizing and modeling mechanical properties of nanocomposites - review and evaluation. *J Miner Mater Charact Eng* 9(4):275–319
- Hu L, Hecht DS, Gruner G (2010b) Carbon nanotube thin films: fabrication, properties, and applications. *Chem Rev* 110(10):5790–5844. <https://doi.org/10.1021/cr9002962>
- Hughes MA, Allen JA, Donne SW (2015) Carbonate reduction and the properties and applications of carbon formed through electrochemical deposition in molten carbonates: a review. *Electrochim Acta* 176:1511–1521. <https://doi.org/10.1016/j.electacta.2015.07.134>
- Iijima S (1991) Helical microtubules of graphitic carbon. *Nature* 354(6348):56–58. <https://doi.org/10.1038/354056a0>
- Iijima S, Ichihashi T (1993) Single-shell carbon nanotubes of 1-nm diameter. *Nature* 363(6430):603–605. <https://doi.org/10.1038/363603a0>
- Ijije HV, Sun C, Chen GZ (2014a) Indirect electrochemical reduction of carbon dioxide to carbon nanopowders in molten alkali carbonates: process variables and product properties. *Carbon* 73:163–174. <https://doi.org/10.1016/j.carbon.2014.02.052>
- Ijije HV, Lawrence RC, Siambun NJ, Jeong SM, Jewell D, Hu D, Chen GZ (2014b) Electrodeposition and re-oxidation of carbon in carbonate-containing molten salts. *Faraday Discuss* 172:105–116. <https://doi.org/10.1039/c4fd00046c>

- Ijije HV, Lawrence R, Chen G (2014c) Carbon electrodeposition in molten salts: electrode reactions and applications. *RSC Adv* 4:35808–35817. <https://doi.org/10.1039/C4RA04629C>
- Ijije HV, Chen G (2016) Electrochemical manufacturing of nanocarbons from carbon dioxide in molten alkali metal carbonate salts: roles of alkali metal cations. *Adv Manuf* 4(1):23–32. <https://doi.org/10.1007/s40436-015-0125-2>
- Ingram MD, Baron B, Janz GJ (1966) The electrolytic deposition of carbon from fused carbonates. *Electrochim Acta* 11(11):1629–1639. [https://doi.org/10.1016/0013-4686\(66\)80076-2](https://doi.org/10.1016/0013-4686(66)80076-2)
- Ito Y, Shimada T, Kawamura H (1992) Electrochemical formation of thin carbon film from molten chloride system. *Proc – Electrochem Soc* 1992-16:574–585. <https://doi.org/>. <https://doi.org/10.1149/199216.0574PV>
- Jacob MV, Rawat RS, Ouyang B, Bazaka K, Kumar DS, Taguchi D, Iwamoto M, Neupane R, Varghese OK (2015) Catalyst-free plasma enhanced growth of graphene from sustainable sources. *Nano Lett* 15(9):5702–5708. <https://doi.org/10.1021/acs.nanolett.5b01363>
- Jiang H, Ni QQ, Wang H, Liu J (2012) Fabrication and characterization of NBR/MWCNT composites by latex technology. *Polym Compos* 33(9):1586–1592. <https://doi.org/10.1002/polb.22297>
- Jiang H, Wei Z, Cai X, Lai L, Ma J, Huang W (2019) A cathode for Li-ion batteries made of vanadium oxide on vertically aligned carbon nanotubes/graphene foam. *Chem Eng J* 359:1668–1696. <https://doi.org/10.1016/j.cej.2018.10.223>
- Kamali AR, Schwandt C, Fray DJ (2011) Effect of the graphite electrode material on the characteristics of molten salt electrolytically produced carbon nanomaterials. *Mater Charact* 62(10):987–994. <https://doi.org/10.1016/j.matchar.2011.06.010>
- Kamali AR, Fray DJ (2013) Molten salt corrosion of graphite as a possible way to make carbon nanostructures. *Carbon* 56:121–131. <https://doi.org/10.1016/j.carbon.2012.12.076>
- Kamo M, Sato Y, Matsumoto S, Setaka N (1983) Diamond synthesis from gas phase in microwave plasma. *J Cryst Growth* 62:642–644. [https://doi.org/10.1016/0022-0248\(83\)90411-6](https://doi.org/10.1016/0022-0248(83)90411-6)
- Kaplan B, Groult H, Barhoun A, Lantelme F, Nakajima T, Gupta V, Komabe S, Kumagai N (2002) Synthesis and structural characterization of carbon powder by electrolytic reduction of molten $\text{Li}_2\text{CO}_3\text{Na}_2\text{CO}_3\text{K}_2\text{CO}_3$. *J Electrochem Soc* 149(5):D72–D78. <https://doi.org/10.1149/1.1464884>
- Karen WMJ, Gakim M, Janaun JA, Liew WYH, Siambun NJ (2018) Effect of temperature and voltage on the preparation of solid carbon by electrolysis of a molten $\text{CaCO}_3\text{-Li}_2\text{CO}_3\text{-LiCl}$ electrolyte. *Int J Electrochem Sci* 13:9771–9783. <https://doi.org/10.20964/2018.10.43>
- Kawamura H, Ito Y (2000) Electrodeposition of cohesive carbon films on aluminum in a $\text{LiCl-KCl-K}_2\text{CO}_3$ melt. *J Appl Electrochem* 30:571–574. <https://doi.org/10.1023/A:1003927100308>
- Ke Q, Wang J (2016) Graphene-based materials for supercapacitor electrodes - a review. *J Mater* 2(1):37–54. <https://doi.org/10.1016/j.jmat.2016.01.001>
- Kim J, Ishihara M, Koga Y, Tsugawa K, Hasegawa M, Iijima S (2011a) Low-temperature synthesis of large-area graphene-based transparent conductive films using surface wave plasma chemical vapor deposition. *Appl Phys Lett* 98:091502. <https://doi.org/10.1063/1.3561747>
- Kim Y, Song W, Lee SY, Jeon C, Jung W, Kim M, Park C-Y (2011b) Low-temperature synthesis of graphene on nickel foil by microwave plasma chemical vapor deposition. *Appl Phys Lett* 98:263106. <https://doi.org/10.1063/1.3605560>
- Kleinsorge B, Golovko VB, Hofmann S, Geng J, Jefferson D, Robertson J, Johnson BFG (2004) Growth of aligned carbon nanofibres over large areas using colloidal catalysts at low temperatures. *Chem Commun*:1416–1417. <https://doi.org/10.1039/B401785D>
- Koo JH (2006) *Polymer nanocomposites: processing, characterization, and applications*. McGraw-Hill, New York
- Krishnamoorthy R, Govindan B, Banat F, Sagadevan V, Purushothaman M, Show PL (2019) Date pits activated carbon for divalent lead ions removal. *J Biosci Bioeng*. <https://doi.org/10.1016/j.jbiosc.2018.12.011>
- Krishnan D, Raidongia K, Shao J, Huang J (2014) Graphene oxide assisted hydrothermal carbonization of carbon hydrates. *ACS Nano* 8(1):449–457. <https://doi.org/10.1021/nn404805p>
- Kroto HW, Heath JR, O'Brien SC, Curl RF, Smalley RE (1985) C₆₀: Buckminsterfullerene. *Nature* 318(6042):162–163. <https://doi.org/10.1038/318162a0>

- Kumar R, Singh RK, Singh DP (2016) Natural and waste hydrocarbon precursors for the synthesis of carbon based nanomaterials: graphene and CNTs. *Renew Sust Energ Rev* 58:976–1006. <https://doi.org/10.1016/j.rser.2015.12.120>
- Kurd SM, Hassanifard S, Hartmann S (2017) Fracture toughness of epoxy-based stepped functionally graded materials reinforced with carbon nanotubes. *Iran Polym J* 26(4):253–260. <https://doi.org/10.1007/s13726-017-0512-6>
- Lantelme F, Kaplan B, Groult H, Devilliers D (1999) Mechanism for elemental carbon formation in molecular ionic liquids. *J Mol Liq* 83:255–269. [https://doi.org/10.1016/S0167-7322\(99\)00090-2](https://doi.org/10.1016/S0167-7322(99)00090-2)
- Le Van K, Groult H, Lantelme F, Dubois M, Avignand D, Tressaud A, Komaba S, Kumagai N, Sigrist S (2009) Electrochemical formation of carbon nano-powders with various porosities in molten alkali carbonates. *Electrochim Acta* 54(19):4566–4573. <https://doi.org/10.1016/j.electacta.2009.03.049>
- Li X-L, Lou T-J, Sun X-M, Li Y-D (2004) Highly sensitive WO_3 hollow sphere gas sensors. *Inorg Chem* 43(17):5442–5449. <https://doi.org/10.1021/ic049522w>
- Lin L, Deng B, Sun J, Peng H, Liu Z (2018) Bridging the gap between reality and ideal in chemical vapor deposition growth of graphene. *Chem Rev* 118(18):9281–9343. <https://doi.org/10.1021/acs.chemrev.8b00325>
- Liu G-J, Fan L-Q, Yu F-D, Wu J-H, Liu L, Qiu Z-Y, Liu Q (2013) Facile one-step hydrothermal synthesis of reduced graphene oxide/ Co_3O_4 composites for supercapacitors. *J Mater Sci* 48:8463–8470. <https://doi.org/10.1007/s10853-013-7663-4>
- Lone MY, Kumar A, Husain S, Zulfeqar M, Husain M (2017) Growth of carbon nanotubes by PECVD and its applications: a review. *Curr Nanosci* 13:536–546. <https://doi.org/10.2174/1573413713666170317150807>
- Lu Y, Zhang S, Yin J, Bai C, Zhang J, Li Y, Yang Y, Ge Z, Zhang M, Wei L, Ma M, Ma Y, Chen Y (2017) Mesoporous activated carbon materials with ultrahigh mesopore volume and effective specific surface area for high performance supercapacitors. *Carbon* 124:64–71. <https://doi.org/10.1016/j.carbon.2017.08.044>
- Lv W, Li Z, Deng Y, Yang QH, Kang F (2016) Graphene-based materials for electrochemical energy storage devices: opportunities and challenges. *Energy Storage Mater* 2:107–138. <https://doi.org/10.1016/j.ensm.2015.10.002>
- Ma H, Li C, Zhang M, Hong J-D, Shi G (2017) Graphene oxide induced hydrothermal carbonization of egg proteins for high-performance supercapacitors. *J Mater Chem A* 5:17040–17047. <https://doi.org/10.1039/c7ta04771a>
- Malik R, Zhang L, McConnell C, Schott M, Hsieh Y-Y, Noga R, Alvarez NT, Shanov V (2017) Three-dimensional, free-standing polyaniline/carbon nanotube composite-based electrode for high-performance supercapacitors. *Carbon* 116:579–590. <https://doi.org/10.1016/j.carbon.2017.02.036>
- Massot L, Chamelot P, Bouyer F, Taxil P (2002) Electrodeposition of carbon films from molten alkaline fluoride media. *Electrochim Acta* 47:1949–1957. [https://doi.org/10.1016/S0013-4686\(02\)00047-6](https://doi.org/10.1016/S0013-4686(02)00047-6)
- Melvin GJH, Ni QQ, Natsuki T (2014a) Electromagnetic wave absorption properties of barium titanate/carbon nanotube hybrid nanocomposites. *J Alloys Compd* 615:84–90. <https://doi.org/10.1016/j.jallcom.2014.06.191>
- Melvin GJH, Ni QQ, Suzuki Y, Natsuki T (2014b) Microwave-absorbing properties of silver nanoparticle/carbon nanotube hybrid nanocomposites. *J Mater Sci* 49(14):5199–5207. <https://doi.org/10.1007/s10853-014-8229-9>
- Melvin GJH, Ni QQ, Natsuki T (2014c) Fabrication and characterization of polymer-based electroactive nanocomposite actuator. *Microelectron Eng* 126:9–12. <https://doi.org/10.1016/j.mee.2014.04.001>
- Melvin GJH, Ni QQ, Natsuki T (2014d) Behavior of polymer-based electroactive actuator incorporated with mild hydrothermally treated CNTs. *Appl Phys A Mater Sci Process* 117(4):2043–2050. <https://doi.org/10.1007/s00339-014-8616-8>

- Melvin GJH, Ni QQ, Natsuki T, Wang Z, Morimoto S, Fujishige M, Takeuchi K, Hashimoto Y, Endo M (2015) Ag/CNT nanocomposites and their single-and double-layer electromagnetic wave absorption properties. *Synth Met* 209:383–388. <https://doi.org/10.1016/j.synthmet.2015.08.017>
- Melvin GJH, Ni QQ, Natsuki T (2016) Bending actuation and charge distribution behavior of polyurethane/carbon nanotube electroactive nanocomposites. *Polym Compos* 37(1):262–269. <https://doi.org/10.1002/pc.23177>
- Melvin GJH, Ni QQ, Wang Z (2017a) Performance of barium titanate@carbon nanotube nanocomposite as an electromagnetic wave absorber. *Phys Status Solidi A* 214(2):1600541. <https://doi.org/10.1002/pssa.201600541>
- Melvin GJH, Wang Z, Siambun NJ, Rahman MM (2017b) Carbon materials derived from rice husks at low and high temperatures. *IOP Conf Ser: Mater Sci Eng* 217:012017. <https://doi.org/10.1088/1757-899X/217/1/012017>
- Melvin GJH, Wang Z, Ni Q-Q, Siambun NJ, Rahman MM (2017c) Electromagnetic wave absorption properties of rice husks carbonized at 2500°C. *AIP Conf Proceed* 1901(1):020002. <https://doi.org/10.1063/1.5010439>
- Melvin GJH, Wang Z, Ni QQ, Siambun NJ, Rahman MM (2017d) Fabrication and characterization of carbonized rice husk/barium titanate nanocomposites. *IOP Conf Ser: Mater Sci Eng* 229:012024. <https://doi.org/10.1088/1757-899X/229/1/012024>
- Melvin GJH, Zhu Y, Ni QQ (2019a) Nanomaterials: electromagnetic wave energy loss. In: Siddiquee S, Melvin GJH, Rahman MM (eds) *Nanotechnology: applications in energy, drug and food*. Springer, Cham, pp 73–97. https://doi.org/10.1007/978-3-319-99602-8_4
- Melvin GJH, Chai KF, Tamiri FM (2019b) Characterization of carbonized waste materials: Rice husk and saw dust. *IOP Conf Ser: Mater Sci Eng* 606:012002. <https://doi.org/10.1088/1757-899X/606/1/012002>
- Melvin GJH, Wang Z, Ni QQ (2019c) Electromagnetic wave absorption performance of carbonized rice husk obtained at various temperatures. *Global Chall* 3(11):1900045. <https://doi.org/10.1002/gch2.201900045>
- Melvin GJH, Wang Z, Morimoto S, Fujishige M, Takeuchi K, Hashimoto Y, Endo M (2019d) Graphite whiskers derived from waste coffee grounds treated at high temperature. *Global Chall* 3(8):1800107. <https://doi.org/10.1002/gch2.201800107>
- Mishra N, Das G, Ansaldo A, Genovese A, Malerba M, Povia M, Ricci D, Di Fabrizio E, Di Zitti E, Sharon M, Sharon M (2012) Pyrolysis of waste polypropylene for the synthesis of carbon nanotubes. *J Anal Appl Pyrolysis* 94:91–98. <https://doi.org/10.1016/j.jaap.2011.11.012>
- Nandamuri G, Roumimov S, Solanki R (2010) Remote plasma assisted growth of graphene films. *Appl Phys Lett* 96:154101. <https://doi.org/10.1063/1.3387812>
- Nasir S, Hussein M, Zainal Z, Yusof N (2018) Carbon-based nanomaterials/allotropes: a glimpse of their synthesis, properties and some applications. *Materials* 11(2):295. <https://doi.org/10.3390/ma11020295>
- Ni QQ, Melvin GJH, Natsuki T (2015) Double-layer electromagnetic wave absorber based on barium titanate/carbon nanotube nanocomposites. *Ceram Int* 41(8):9885–9892. <https://doi.org/10.1016/j.ceramint.2015.04.065>
- Nizamuddin S, Baloch HA, Griffin GJ, Mubarak NM, Bhutto AW, Abro R, Mazari SA, Ali BS (2017) An overview of effect of process parameters on hydrothermal carbonization of biomass. *Renew Sust Energ Rev* 73:1289–1299. <https://doi.org/10.1016/j.rser.2016.12.122>
- Novoselov KS, Geim AK, Morozov SV, Jiang D, Zhang Y, Dubonos SV, Grigorieva IV, Firsov AA (2004) Electric field effect in atomically thin carbon films. *Science* 306(5696):666–669. <https://doi.org/10.1126/science.1102896>
- Novoselova IA, Oliinyk NF, Volkov SV, Konchits AA, Yanchuk IB, Yefanov VS, Kolesnik SP, Karpets MV (2008) Electrolytic synthesis of carbon nanotubes from carbon dioxide in molten salts and their characterization. *Phys E* 40(7):2231–2237. <https://doi.org/10.1016/j.physe.2007.10.069>

- Nwigboji IH, Ejembi JI, Wang Z, Bagayoko D, Zhao GL (2015) Microwave absorption properties of multi-walled carbon nanotube (outer diameter 20–30 nm)-epoxy composites from 1 to 26.5 GHz. *Diam Relat Mater* 52:66–71. <https://doi.org/10.1016/j.diamond.2014.12.008>
- Ober CK, Müllen K (2012) Introduction – applications of polymers. In: Krzysztof Matyjaszewski K, Möller M (eds) *Polymer science: a comprehensive reference*. Elsevier, Amsterdam, pp 439–478
- Oberlin A, Endo M, Koyama T (1976) Filamentous growth of carbon through benzene decomposition. *J Cryst Growth* 32(3):335–349. [https://doi.org/10.1016/0022-0248\(76\)90115-9](https://doi.org/10.1016/0022-0248(76)90115-9)
- Omoriyekomwan JE, Tahmasebi A, Zhang J, Yu J (2017) Formation of hollow carbon nanofibers on bio-char during microwave pyrolysis of palm kernel shell. *Energy Convers Manag* 148:583–592. <https://doi.org/10.1016/j.enconman.2017.06.022>
- Pan D, Zhang J, Li Z, Wu M (2010) Hydrothermal route for cutting graphene sheets into blue-luminescent graphene quantum dots. *Adv Mater* 22:734–738. <https://doi.org/10.1002/adma.200902825>
- Papageorgiou DG, Kinloch IA, Young RJ (2015) Graphene/elastomer nanocomposites. *Carbon* 95:460–484. <https://doi.org/10.1016/j.carbon.2015.08.055>
- Popov VN (2004) Carbon nanotubes: properties and application. *Mater Sci Eng R* 43(3):61–102. <https://doi.org/10.1016/j.mser.2003.10.001>
- Potts JR, Dreyer DR, Bielawski CW, Ruoff RS (2011) Graphene-based polymer nanocomposites. *Polymer* 52(1):5–25. <https://doi.org/10.1016/j.polymer.2010.11.042>
- Pumera M (2010) Graphene-based nanomaterials and their electrochemistry. *Chem Soc Rev* 39(11):4146–4157. <https://doi.org/10.1039/c002690p>
- Purkait T, Singh G, Singh M, Kumar D, Dey RS (2017) Large area few-layer graphene with scalable preparation from waste biomass for high-performance supercapacitor. *Sci Rep* 7(1):15239. <https://doi.org/10.1038/s41598-017-15463-w>
- Qian H-S, Yu S-H, Luo L-B, Gong J-Y, Fei L-F, Liu X-M (2006) Synthesis of uniform Te@carbon-rich composite nanocables with photoluminescence properties and carbonaceous nanofibers by hydrothermal carbonization of glucose. *Chem Mater* 18:2102–2101. <https://doi.org/10.1021/cm052848y>
- Qiu J, Qiu T (2015) Fabrication and microwave absorption properties of magnetite nanoparticle–carbon nanotube–hollow carbon fiber composites. *Carbon* 81:20–28. <https://doi.org/10.1016/j.carbon.2014.09.011>
- Raghavan N, Thangavel S, Venugopal G (2017) A short review on preparation of graphene from waste and bioprecursors. *Appl Mater Today* 7:246–254. <https://doi.org/10.1016/j.apmt.2017.04.005>
- Randviir EP, Brownson DA, Banks CE (2014) A decade of graphene research: production, applications and outlook. *Mater Today* 17(9):426–432. <https://doi.org/10.1016/j.mattod.2014.06.001>
- Ren J, Li FF, Lau J, González-Urbina L, Licht S (2015) One-pot synthesis of carbon Nanofibers from CO₂. *Nano Lett* 15(9):6142–6148. <https://doi.org/10.1021/acs.nanolett.5b02427>
- Ren ZF, Huang ZP, Xu JW, Wang JH, Bush P, Siegal MP, Provencio PN (1998) Synthesis of large arrays of well-aligned carbon nanotubes on glass. *Science* 282:1105–1107. <https://doi.org/10.1126/science.282.5391.1105>
- Rosmi MS, Shinde SM, Rahman ND, Thangaraja A, Sharma S, Sharma KP, Yaakob Y, Vishwakarma RK, Bakar SA, Kalita G, Ohtani H, Tanemura M (2016) Synthesis of uniform monolayer graphene on re-solidified copper from waste chicken fat by low pressure chemical vapor deposition. *Mater Res Bull* 83:573–580. <https://doi.org/10.1016/j.materresbull.2016.07.010>
- Ruan G, Sun Z, Peng Z, Tour JM (2011) Growth of graphene from food, insects, and waste. *ACS Nano* 5(9):7601–7607. <https://doi.org/10.1021/nn202625c>
- Saghafi M, Mahboubi F, Mohajezaden S, Holze R (2014) Preparation of vertically aligned carbon nanotubes and their electrochemical performance in supercapacitors. *Synth Met* 195:252–259. <https://doi.org/10.1016/j.synthmet.2014.06.012>

- Sahoo NG, Jung YC, Yoo HJ, Cho JW (2007) Influence of carbon nanotubes and polypyrrole on the thermal, mechanical and electroactive shape-memory properties of polyurethane nanocomposites. *Compos Sci Technol* 67(9):1920–1929. <https://doi.org/10.1016/j.compscitech.2006.10.013>
- Saito Y, Arima T (2007) Features of vapor-grown cone-shaped graphitic whiskers deposited in the cavities of wood cells. *Carbon* 45(2):248–255. <https://doi.org/10.1016/j.carbon.2006.10.002>
- Sajjadi SA, Meknati A, Lima EC, Dotto GL, Mendoza-Castillo DI, Anastopoulos I, Alakhras F, Unuabonah EI, Singh P, Hosseini-Bandegharai A (2019) A novel route for preparation of chemically activated carbon from pistachio wood for highly efficient Pb (II) sorption. *J Environ Manag* 236:34–44. <https://doi.org/10.1016/j.jenvman.2019.01.087>
- Satayeva AR, Howell CA, Korobeinyk AV, Jandosov J, Inglezakis VJ, Mansurov ZA, Mikhailovsky SV (2018) Investigation of rice husk derived activated carbon for removal of nitrate contamination from water. *Sci Total Environ* 630:1237–1245. <https://doi.org/10.1016/j.scitotenv.2018.02.329>
- Schaefer DW, Justice RS (2007) How nano are nanocomposites? *Macromolecules* 40(24):8501–8517. <https://doi.org/10.1021/ma070356w>
- Schwander M, Partes K (2011) A review of diamond synthesis by CVD processes. *Dia Relat Mater* 20(9):1287–1301. <https://doi.org/10.1016/j.diamond.2011.08.005>
- Seo DH, Han ZJ, Kumar S, Ostrikov K (2013a) Structure-controlled, vertical graphene-based, binder-free electrodes from plasma-reformed butter enhance supercapacitor performance. *Adv Energy Mater* 3(10):1316–1323. <https://doi.org/10.1002/aenm.201300431>
- Seo DH, Rider AE, Han ZJ, Kumar S, Ostrikov K (2013b) Plasma break-down and re-bulid: same functional vertical graphenes from diverse natural precursors. *Adv Mater* 25(39):5638–5642. <https://doi.org/10.1002/adma.201301510>
- Sevilla M, Lota G, Fuertes AB (2007) Saccharide-based graphitic carbon nanocoils as supports for PtRu nanoparticles for methanol electrooxidation. *J Power Sources* 171:546–551. <https://doi.org/10.1016/j.jpowsour.2007.05.096>
- Sevilla M, Fuertes AB (2009a) Chemical and structural properties of carbonaceous products obtained by hydrothermal carbonization of saccharides. *Chem Eur J* 15:4195–4203. <https://doi.org/10.1002/chem.200802097>
- Sevilla M, Fuertes AB (2009b) The production of carbon materials by hydrothermal carbonization of cellulose. *Carbon* 47:2281–2289. <https://doi.org/10.1016/j.carbon.2009.04.026>
- Shams SS, Zhang LS, Hu R, Zhang R, Zhu J (2015) Synthesis of graphene from biomass: a green chemistry approach. *Mater Lett* 161:476–479. <https://doi.org/10.1016/j.matlet.2015.09.022>
- Sharma S, Kalita G, Hirano R, Shinde SM, Papon R, Ohtani H, Tanemura M (2014) Synthesis of graphene crystals from solid waste plastic by chemical vapor deposition. *Carbon* 72:66–73. <https://doi.org/10.1016/j.carbon.2014.01.051>
- Shen J, Yan B, Shi M, Ma H, Li N, Ye M (2011) One step hydrothermal synthesis of TiO₂-reduced graphene oxide sheets. *J Mater Chem* 21:3415–3421. <https://doi.org/10.1039/C0JM03542D>
- Shrestha S, Choi WC, Song W, Kwon YT, Shrestha SP, Park C-Y (2010) Preparation and field emission properties of Er-decorated multiwalled carbon nanotubes. *Carbon* 48(1):54–59. <https://doi.org/10.1016/j.carbon.2009.08.029>
- Silberberg MS (2006) *Chemistry: the molecular nature of matter and change*. McGraw Hill, Boston
- Song C (2002) CO₂ conversion and utilization : an overview. In: Song C, Gaffney AF, Fujimoto K (eds) CO₂ conversion and utilization. ACS Symp Ser 809:2–30. <https://doi.org/10.1021/bk-2002-0809.ch001>
- Song Q, Xu Q, Wang Y, Shang X, Li Z (2012) Electrochemical deposition of carbon films on titanium in molten LiCl–KCl–K₂CO₃. *Thin Solid Films* 520(23):6856–6863. <https://doi.org/10.1016/j.tsf.2012.07.056>
- Styring P, Jansen D, De Coninck H, Reith H, Armstrong K (2011) Carbon capture and utilisation in the green economy. Centre for Low Carbon Futures
- Stuardi FM, Macpherson F, Leclair J (2019) Integrated CO₂ capture and utilization : a priority research direction. *Curr Opin Green Sustainable Chem* 16:71–76. <https://doi.org/10.1016/j.cogsc.2019.02.003>

- Sun X, Li Y (2004a) Colloidal carbon spheres and their core/shell structures with noble-metal nanoparticles. *Angew Chem* 116:607–611. <https://doi.org/10.1002/ange.200352386>
- Sun X, Li Y (2004b) Ga₂O₃ and GaN semiconductor hollow spheres. *Angew Chem Int Ed* 43(29):3827–3831. <https://doi.org/10.1002/anie.200353212>
- Tang D, Yin H, Mao X, Xiao W, Wang DH (2013) Effects of applied voltage and temperature on the electrochemical production of carbon powders from CO₂ in molten salt with an inert anode. *Electrochim Acta* 114:567–573. <https://doi.org/10.1016/j.electacta.2013.10.109>
- Thostenson ET, Li C, Chou TW (2005) Nanocomposites in context. *Compos Sci Technol* 65:491–516. <https://doi.org/10.1016/j.compscitech.2004.11.003>
- Thostenson ET, Ren Z, Chou TW (2001) Advances in the science and technology of carbon nanotubes and their composites: a review. *Compos Sci Technol* 61(13):1899–1912. [https://doi.org/10.1016/S0266-3538\(01\)00094-X](https://doi.org/10.1016/S0266-3538(01)00094-X)
- Titirici MM, White RJ, Brun N, Budarin VL, Su DS, del Monte F, Clark JH, MacLachlan MJ (2015) Sustainable carbon materials. *Chem Soc Rev* 44(1):250–290. <https://doi.org/10.1039/c4cs00232f>
- Van Krevelen DW (1950) Graphical-statistical method for the study of structure and reaction processes of coal. *Fuel* 29:269–228
- Wang E, Dong Y, Islam MZ, Yu L, Liu F, Chen S, Qi X, Zhu Y, Fu Y, Xu Z, Hu N (2019a) Effect of graphene oxide-carbon nanotube hybrid filler on the mechanical property and thermal response speed of shape memory epoxy composites. *Compos Sci Technol* 169:209–216. <https://doi.org/10.1016/j.compscitech.2018.11.022>
- Wang Z, Melvin GJH (2019) Carbon nanomaterials for energy storage devices. In: Siddiquee S, Melvin GJH, Rahman MM (eds) *Nanotechnology: applications in energy, drug and food*. Springer, Cham, pp 1–29. https://doi.org/10.1007/978-3-319-99602-8_1
- Wang Y, Wang J, Morimoto S, Melvin GJH, Zhao R, Hashimoto Y, Terrones M (2019c) Nitrogen-doped porous carbon monoliths from molecular-level dispersion of carbon nanotubes into polyacrylonitrile (PAN) and the effect of carbonization process for supercapacitors. *Carbon* 143:776–785. <https://doi.org/10.1016/j.carbon.2018.11.024>
- Wang Q, Li H, Chen L, Huang X (2001) Monodispersed hard carbon spherules with uniform nanopores. *Carbon* 39(14):2211–2214. [https://doi.org/10.1016/S0008-6223\(01\)00040-9](https://doi.org/10.1016/S0008-6223(01)00040-9)
- Wang H, Abe T, Maruyama S, Iriyama Y, Ogumi Z, Yoshikawa K (2005) Graphitized carbon nanobeads with an onion texture as lithium-ion battery negative electrode for high-rate use. *Adv Mater* 17:2857–2860. <https://doi.org/10.1002/adma.200500320>
- Wang C, Xiangfeng C, Mingmei W (2007) Highly sensitive gas sensors based on hollow SnO₂ spheres prepared by carbon sphere template method. *Sens Actuators B: Chem* 120(2):508–513. <https://doi.org/10.1016/j.snb.2006.03.004>
- Wang L, Guo Y, Zhu Y, Li Y, Qu Y, Rong C, Ma X, Wang Z (2010) A new route for preparation of hydrochars from rice husk. *Bioresour Technol* 101(24):9807–9810. <https://doi.org/10.1016/j.biortech.2010.07.031>
- Wang Z, Shoji M, Ogata H (2011a) Carbon nanosheets by microwave plasma enhanced chemical vapor deposition in CH₄-Ar system. *Appl Surf Sci* 257:9082–9085. <https://doi.org/10.1016/j.apsusc.2011.05.104>
- Wang Z, Shoji M, Ogata H (2011b) Facile low-temperature growth of carbon nanosheets toward simultaneous determination of dopamine, ascorbic acid and uric acid. *Analyst* 136:4903–4905. <https://doi.org/10.1039/c1an15630f>
- Wang Z, Shoji M, Ogata H (2012a) Electrochemical determination of NADH based on MPECVD carbon nanosheets. *Talanta* 99:487–491. <https://doi.org/10.1016/j.talanta.2012.06.014>
- Wang Z, Shoji M, Ogata H (2012b) Synthesis and characterization of platinum nanoparticles on carbon nanosheets with enhanced electrocatalytic activity towards methanol oxidation. *Appl Surf Sci* 259:219–224. <https://doi.org/10.1016/j.apsusc.2012.07.022>
- Wang Z, Ogata H, Morimoto S, Fujishige M, Takeuchi K, Hashimoto Y, Endo M (2014a) Synthesis of carbon nanosheets from Kapton polyimide by microwave plasma treatment. *Carbon* 72:421–424. <https://doi.org/10.1016/j.carbon.2014.02.021>

- Wang Z, Shoji M, Baba K, Ito T, Ogata H (2014b) Microwave plasma-assisted regeneration of carbon nanosheets with bi- and trilayer of graphene and their application to photovoltaic cells. *Carbon* 67:326–335. <https://doi.org/10.1016/j.carbon.2013.10.002>
- Wang Z, Ogata H, Morimoto S, Fujishige M, Takeuchi K, Hashimoto Y, Endo M (2015a) High-temperature-induced growth of graphite whiskers from fullerene waste soot. *Carbon* 90:154–159. <https://doi.org/10.1016/j.carbon.2015.04.017>
- Wang Z, Ogata H, Morimoto S, Oritz-Medina J, Fujishige M, Takeuchi K, Muramatsu H, Hayashi T, Terrones M, Hashimoto Y, Endo M (2015b) Nanocarbons from rice husks by microwave plasma irradiation: from graphene and carbon nanotubes to graphenated carbon nanotube hybrids. *Carbon* 94:479–484. <https://doi.org/10.1016/j.carbon.2015.07.037>
- Wang Z, Ogata H, Morimoto S, Fujishige M, Takeuchi K, Muramatsu H, Hayashi T, Oritz-Medina J, Yusop MZM, Tanemura M, Terrones M, Hashimoto Y, Endo M (2015c) Microwave plasma-induced graphene-sheet fibers from waste coffee grounds. *J Mater Chem A* 3:14545–14549. <https://doi.org/10.1039/c5ta03833b>
- Wang Z, Ogata H, Melvin GJH, Obata M, Morimoto S, Ortiz-Medina J, Cruz-Silva R, Fujishige M, Takeuchi K, Muramatsu H, Kim TY, Kim YA, Hayashi T, Terrones M, Hashimoto Y, Endo M (2017) Structural evolution of hydrothermal carbon spheres induced by high temperatures and their electrical properties under compression. *Carbon* 121:426–433. <https://doi.org/10.1016/j.carbon.2017.06.003>
- Wei L, Yushin G (2012) Nanostructured activated carbons from natural precursors for electrical double layer capacitors. *Nano Energy* 1(4):552–565. <https://doi.org/10.1016/j.nanoen.2012.05.002>
- Wu A, Yan J, Xu W, Li X (2016a) Fabrication of waste biomass derived carbon by pyrolysis. *Mat Lett* 173:60–63. <https://doi.org/10.1016/j.matlet.2016.03.025>
- Wu H, Li Z, Ji D, Liu Y, Li L, Yuan D, Zhang Z, Ren J, Lefler M, Wang B, Licht S (2016b) One-pot synthesis of nanostructured carbon materials from carbon dioxide via electrolysis in molten carbonate salts. *Carbon* 106:208–217. <https://doi.org/10.1016/j.carbon.2016.05.031>
- Xu Y, Sheng K, Li C, Shi G (2010) Self-assembled graphene hydrogel via a one-step hydrothermal process. *ACS Nano* 4:4324–4330. <https://doi.org/10.1021/nn101187z>
- Yan Y, Xia H, Qiu Y, Xu Z, Ni QQ (2019) Multi-layer graphene oxide coated shape memory polyurethane for adjustable smart switches. *Compos Sci Technol* 172:108–116. <https://doi.org/10.1016/j.compscitech.2019.01.013>
- Yan J, Zhang Z (2019) Carbon capture, utilization and storage (CCUS). *Appl Energy* 235:1289–1299. <https://doi.org/10.1016/j.apenergy.2018.11.019>
- Yang Z-C, Zhang Y, Kong J-H, Wong SY, Li X, Wang J (2013) Hollow carbon nanoparticles of tunable size and wall thickness by hydrothermal treatment of α -cyclodextrin template by F127 block copolymers. *Chem Mater* 25:704–710. <https://doi.org/10.1021/cm303513y>
- Yin H, Mao X, Tang D, Xiao W, Xing L, Zhu H, Wang D, Sadoway DR (2013) Capture and electrochemical conversion of CO₂ to value-added carbon and oxygen by molten salt electrolysis. *Energy Environ Sci* 6(5):1538–1545. <https://doi.org/10.1039/c3ee24132g>
- Young RJ, Lovell PA (2011) Introduction to polymers. CRC Press, Boca Raton
- Yu K, Lu G, Bo Z, Mao S, Chen J (2011) Carbon nanotubes with chemically bonded graphene leaves for electronic and optoelectronic applications. *J Phys Chem Lett* 2:1556–1562. <https://doi.org/10.1021/jz200641c>
- Yuan Z, Eden MR, Gani R (2016) Towards the development and deployment of large-scale carbon dioxide capture and conversion processes. *Ind Eng Chem Res* 55(12):3383–3419. <https://doi.org/10.1021/acs.iecr.5b03277>
- Zanin H, May PW, Hamanaka MHMO, Corat EJ (2013) Field emission from hybrid diamond-like carbon and carbon nanotube composite structures. *ACS Appl Mater Interfaces* 5(23):12238–12243. <https://doi.org/10.1021/am403386a>
- Zhang B, Bai S, Cheng H-M, Cai Q-K (2006) Graphitization-induced microstructural changes in tetrahydrofuran-derived pyrolytic carbon spheres. *J Mater Res* 21(9):2198–2203. <https://doi.org/10.1557/jmr.2006.0292>

- Zhang J, Li C, Peng Z, Liu Y, Zhang J, Liu Z, Li D (2017) 3D free-standing nitrogen-doped reduced graphene oxide aerogel as anode material for sodium ion batteries with enhanced sodium storage. *Sci Rep* 7:4886. <https://doi.org/10.1038/s41598-017-04958-1>
- Zhang J, Tahmasebi A, Omoriyekomwan JE, Yu J (2018) Direct synthesis of hollow carbon nanofibers on bio-char during microwave pyrolysis of pine nut shell. *J Anal Appl Pyrolysis* 130:142–148. <https://doi.org/10.1016/j.jaap.2018.01.016>
- Zhang L, Ni QQ, Shiga A, Natsuki T, Fu Y (2011) Preparation of polybenzimidazole/function-alized carbon nanotube nanocomposite films for use as protective coatings. *Polym Eng Sci* 51(8):1525–1532. <https://doi.org/10.1002/pen.21618>
- Zhang X, Zhang R, Xiang C, Liu Y, Zou Y, Chu H, Qiu S, Xu F, Sun L (2019) Polydopamine-assisted formation of Co_3O_4 -nanocube-anchored reduced graphene oxide composite for high-performance supercapacitors. *Ceram Int*. <https://doi.org/10.1016/j.ceramint.2019.04.087>
- Zhao B, Liu P, Jiang Y, Pan D, Tao H, Song J, Fang T, Xu W (2012) Supercapacitor performance of thermally reduced graphene oxide. *J Power Sources* 1998:423–427. <https://doi.org/10.1016/j.jpowsour.2011.09.074>
- Zhou M, Zhai YM, Dong SJ (2009) Electrochemical sensing and biosensing platform based on chemically reduced graphene oxide. *Anal Chem* 81(14):5603–5613. <https://doi.org/10.1021/ac900136z>
- Zhu J, Jia J, Kwong FL, Ng DH, Tjong SC (2012) Synthesis of multiwalled carbon nanotubes from bamboo charcoal and the roles of minerals on their growth. *Biomass Bioenergy* 36:12–19. <https://doi.org/10.1016/j.biombioe.2011.08.023>
- Zhu S, Xing C, Wu F, Zuo X, Zhang Y, Yu C, Chen M, Li W, Li Q, Liu L (2019) Cake-like flexible carbon nanotubes/graphene composite prepared via a facile method for high-performance electromagnetic interference shielding. *Carbon* 145:259–265. <https://doi.org/10.1016/j.carbon.2019.01.030>